The hedgehog-PKA pathway regulates two distinct steps of the differentiation of retinal ganglion cells: the cell-cycle exit of retinoblasts and their neuronal maturation

Ichiro Masai[1,*], Masahiro Yamaguchi[1], Noriko Tonou-Fujimori[1], Atsuko Komori[1] and Hitoshi Okamoto[2]

[1]Masai Initiative Research Unit, RIKEN (The Institute of Physical and Chemical Research), 2-1 Hirowasa, Wako-shi, Saitama 351-0198, Japan
[2]Laboratory for Developmental Gene Regulation, RIKEN Brain Science Institute, 2-1 Hirowasa, Wako-shi, Saitama 351-0198, Japan
*Author for correspondence (e-mail: imasai@postman.riken.jp)

Accepted 26 January 2005

Development 132, 1539-1553
Published by The Company of Biologists 2005
doi:10.1242/dev.01714

Summary

In the developing zebrafish retina, neurogenesis is initiated in cells adjacent to the optic stalk and progresses to the entire neural retina. It has been reported that hedgehog (Hh) signalling mediates the progression of the differentiation of retinal ganglion cells (RGCs) in zebrafish. However, the progression of neurogenesis seems to be only mildly delayed by genetic or chemical blockade of the Hh signalling pathway. Here, we show that cAMP-dependent protein kinase (PKA) effectively inhibits the progression of retinal neurogenesis in zebrafish. Almost all retinal cells continue to proliferate when PKA is activated, suggesting that PKA inhibits the cell-cycle exit of retinoblasts. A cyclin-dependent kinase (cdk) inhibitor p27 inhibits the PKA-induced proliferation, suggesting that PKA functions upstream of cyclins and cdk inhibitors. Activation of the Wnt signalling pathway induces the hyperproliferation of retinal cells in zebrafish. The blockade of Wnt signalling inhibits the PKA-induced proliferation, but the activation of Wnt signalling promotes proliferation even in the absence of PKA activity. These observations suggest that PKA inhibits exit from the Wnt-mediated cell cycle rather than stimulates Wnt-mediated cell-cycle progression. PKA is an inhibitor of Hh signalling, and Hh signalling molecule morphants show severe defects in cell-cycle exit of retinoblasts. Together, these data suggest that Hh acts as a short-range signal to induce the cell-cycle exit of retinoblasts. The pulse inhibition of Hh signalling revealed that Hh signalling regulates at least two distinct steps of RGC differentiation: the cell-cycle exit of retinoblasts and RGC maturation. This dual requirement of Hh signalling in RGC differentiation implies that the regulation of a neurogenic wave is more complex in the zebrafish retina than in the *Drosophila* eye.

Key words: cAMP-dependent protein kinase, Cyclin D, *Danio rerio*, p27, Wnt, Zebrafish

Introduction

The vertebrate retina consists of six major classes of neurons and one class of glial cells, which are organized into distinct layers (Dowling, 1987). In the vertebrate retina, neuroepithelial cells are initially mitotic and undergo cell division to generate two mitotic daughter cells. At the stage when neuronal differentiation occurs, progenitor cells start cell division, producing postmitotic progenies, which exit from the cell cycle and differentiate into retinal neurons or glial cells. Cell fate decisions in the developing retina are independent of cell lineage; therefore it seems likely that multipotent progenitor cells change their competence to generate different retinal cell types in response to position and stage-dependent environmental cues (Livesey and Cepko, 2001; Marquardt and Gruss, 2002). Although the generation of postmitotic neuronal progenies, referred to as 'neuronal production' in this paper, is the first step of neuronal differentiation, it is still unclear how mitotic retinoblasts determine when they generate postmitotic progenies.

In all cell types, progression of the cell cycle is regulated by different combinations of cyclins and cyclin-dependent kinases (cdks) (Murray, 2004). Cyclin D1 is expressed abundantly in the developing retina and is important for progression of the cell cycle in vertebrates (Sicinski et al., 1995; Fantl et al., 1995), including in zebrafish (Yarden et al., 1995). Three major types of cdk inhibitor, Cip/Waf, Kip and INK4 family proteins, are important regulators of exit from the cell cycle (Galderisi et al., 2003). Among these, a Kip family protein, p27, is expressed in the developing retina and plays a role in the exit of retinal progenitor cells from the cell cycle by the inhibition of cyclin D1 (Dyer and Cepko, 2001; Geng et al., 2001). Several cell-extrinsic and -intrinsic factors regulating the cell cycle have been identified (Ohnuma and Harris, 2003; Levine and Green, 2004; Yang, 2004). Wnt and Notch (N) are cell-extrinsic regulators of the cell cycle that function upstream of cyclin D and p27 (van Es et al., 2003; Radtke and Raj, 2003). In the chick retina, a Wnt family protein, Wnt2b, is expressed in mitotic progenitor cells and promotes cell proliferation (Kubo et al., 2003). There were reports that cyclin D1 is a target of β-catenin/LEF-1, components of canonical Wnt signalling

(Tetsu and McCormick, 1999; Shtutman et al., 1999). N signalling promotes the exit of retinal progenitor cells from the cell cycle in *Xenopus* retinas (Ohnuma et al., 2002), although N plays a role in the maintenance of neural stem cells in the brain (Radtke and Raj, 2003). Although these factors have been identified, mechanisms underlying the exit of retinal progenitor cells from the cell cycle still remain to be elucidated.

In zebrafish, postmitotic cells are initially generated in the ventronasal retina adjacent to the optic stalk, and neuronal production progresses to the entire neural retina (Hu and Easter, 1999). Our previous study revealed that neuronal production is initiated by the interaction between the optic stalk and the neural retina, and that its progression to the entire neural retina is regulated by the relay of short-range signalling (Masai et al., 2000). The progression of differentiation of retinal ganglion cells (RGCs) and photoreceptors in the zebrafish retina requires the signalling molecule Hedgehog (Hh) (Neumann and Nuesslein-Volhard, 2000; Stenkamp et al., 2000) (reviewed by Russell, 2003; Pujic and Malicki, 2004). These observations raise the possibility that Hh signalling is a candidate for the short-range signalling required for neuronal production. However, the most recent study demonstrated that the expression of *ath5*, one of earliest markers of neuronal production, is suppressed in only 20% of embryos treated with the Hh inhibitor cyclopamine (Stenkamp and Frey, 2003). Furthermore, the suppression of *ath5* expression occurs only following treatment with cyclopamine before invagination of the optic cup, and the progression of *ath5* expression is slightly delayed by the treatment with cyclopamine from the stage when Hh is expressed in the retina. Thus, Stenkamp and Frey predicted that both the initial induction and early progression of *ath5* expression may be regulated by long-range Hh-dependent midline signalling, and that short-range Hh signalling within the neural retina plays only a supplemental role in the progression of *ath5* expression (Stenkamp and Frey, 2003). Thus, it is still unclear whether Hh signalling essentially regulates the progression of *ath5* expression and neuronal production.

Much of our knowledge about the mechanisms underlying the Hh signalling pathway is based on its genetic studies in *Drosophila* (reviewed by Ingham and McMahon, 2001; Cohen, 2003). Hh is released from secreting cells and binds to the receptor protein Patched (Ptc) in responding cells, thereby relieving the Ptc-mediated inhibition of Smoothened (Smo), a seven transmembrane protein essential for the transduction of all Hh-signalling activity. Activated Smo signals to the transcription factor Cubitus interruptus (Ci), which acts as a bipotential transcription factor that can repress, as well as activate, Hh target genes. In the absence of Hh signalling, the repressor form is generated by proteolytic cleavage of full-length protein, which is promoted by cAMP-dependent protein kinase (PKA)-mediated phosphorylation. In the presence of Hh signalling, the cleavage of Ci is inhibited and a full-length activator isoform predominates. It is the balance between these activator and repressor forms of Ci that determines the specific target genes that the cell expresses in response to a particular level of Hh-signalling activity. In vertebrates, at least three Ci homologous genes called Gli, Gli1, Gli2 and Gli3, mediate the transcriptional response to Hh signals. Less is known about Gli family functions than is known about Ci function. Gli1 does not undergo preteolytic cleavage and appears to be solely an activator of the Hh response. Gli2 and possibly Gli3 have both activator and repressor forms, although the in vivo cleavage of these proteins has not been directly demonstrated. In vertebrates, the activity of the Gli transcription factors is negatively regulated by PKA (Hammerschmidt et al., 1996), which possibly acts to promote the cytoplasmic sequestration of Gli1 and generate the repressor forms of Gli2 and Gli3.

Here we show that forskolin treatment effectively inhibits the progression of neuronal production in the zebrafish retina. In the presence of forskolin, a few postmitotic cells are generated adjacent to the optic stalk, but neuronal production is completely inhibited in the remaining region of the neural retina. Forskolin activates adenynyl cyclase, which increases the level of cAMP and then the activity of PKA. The introduction of a dominant-negative form of PKA (dnPKA) rescues the progression of neuronal production in the presence of forskolin. These data clearly show that the initial induction of neurogenesis in the ventronasal retina is PKA-independent, and that the activation of PKA strongly inhibits the progression of retinal neurogenesis. In the presence of forskolin, almost all retinal cells fail to exit from the cell cycle but instead continue to proliferate, suggesting that PKA inhibits the cell-cycle exit of retinal progenitor cells. The introduction of a cdk inhibitor, p27, inhibits cell-cycle progression even in the presence of forskolin, suggesting that PKA functions upstream of p27. Blockade of Wnt signalling also inhibits cell-cycle progression in forskolin-treated retinas. However, the activation of Wnt signalling promotes the cell-cycle progression even in the absence of PKA activity. These observations suggest that Wnt activation is sufficient to maintain proliferation regardless of the level of PKA activity, and that PKA seems to inhibit exit from the Wnt-mediated cell cycle rather than stimulate Wnt-mediated cell-cycle progression. Cell-cycle exit of retinoblasts is similarly affected by blockade of the Hh signalling pathway. Together, these data suggest that Hh signalling regulates the progression of neuronal production.

In *Drosophila*, Hh is activated in differentiating photoreceptors and acts on adjacent uncommitted cells causing them to differentiate into photoreceptors, which in turn become a new source of Hh signals (Kumar, 2001). Zebrafish *sonic hh* (*shh*) and *tiggy-winkle hh* (*twhh*) are expressed in RGCs and induce RGC differentiation non-cell-autonomously (Neumann and Nuesslein-Volhard, 2000), raising the possibility that Hh emanating from RGCs induces neighbouring progenitor cells to generate postmitotic cells, which in turn become a source of Hh signals. However, pulse treatment with forskolin shows that Hh regulates at least two distinct steps of RGC differentiation: cell-cycle exit of retinoblasts and progression of postmitotic cells into mature RGCs. This dual requirement of Hh signalling implies that the mechanism underlying a neurogenic wave in the zebrafish retina is more complex than that in the *Drosophila* eye.

Materials and methods

Fish

Zebrafish (*Danio rerio*) were maintained at 28.5°C on a 14-hour light/10-hour dark cycle. Embryos were collected by natural spawning. The smu^{b577} alleles were used (Varga et al., 2001). Two transgenic strains carrying the green fluorescent protein (GFP) under the control of *ath5* (Masai et al., 2003) and *shh* retinal enhancers

(Neumann and Nuesslein-Volhard, 2000) were used; they are referred to as Tg(ath5:GFP) and Tg(shh:GFP), respectively, in this paper. The TOPdGFP transgenic line (Dorsky et al., 2002) carries GFP under the control of a β-catenin-responsive promoter and was used to monitor the activation of canonical Wnt signalling.

The treatment with forskolin and cyclopamine

Embryos were treated with forskolin according to the procedure previously described (Barresi et al., 2000). As Hh-dependent midline signalling promotes the fate of the optic stalk and represses that of the neural retina (Macdonald et al., 1995), forskolin treatment from early stages causes the cyclopia phenotype (Barresi et al., 2000). To prevent this defect, forskolin was applied to embryos after the regional specification of the optic cup, by midline signalling, is completed. All treatments with forskolin in this study were carried out from 18 hours postfertilisation (hpf), except the pulse treatment shown in Fig. 6. According to the previous study (Neumann and Nuesslein-Volhard, 2000), cyclopamine (TRC Biomedical Research Chemicals, New York, Ontario, Canada) was dissolved in ethanol and diluted to a final concentration of 100 μM for use. We also used cyclopamine-KAAD (Calbiochem) at a final concentration of 75 μM.

In situ hybridisation, antibody labelling, plastic sectioning and cell transplantation

Whole-mount in situ hybridisation, antibody labelling, plastic sectioning and cell transplantation were performed as described previously (Masai et al., 2003). Antibody labelling was carried out using an anti-phosphorylated histone H3 antibody (Upstate Biotechnology) at 1:500, an anti-tubulin antibody (Sigma) at 1:1000, an anti-myc antibody (CALBIOCEM) at 1:200, an anti-bromodeoxyuridine (BrdU) antibody (Roche) at 1:100, an anti-CREB antibody (Cell signaling) at 1:1000, an anti-phosphorylated CREB antibody (Ser133) (Cell signaling) at 1:1000, and an Alexa-532-conjugated anti-mouse or anti-rabbit IgG antibody (Molecular Probes) at 1:500.

BrdU incorporation

Dechorionated embryos were soaked for 30 minutes in Ringer's solution containing 10 mM BrdU (Sigma) and 15% dimethyl sulfoxide (DMSO) at 6°C. After BrdU treatment, the embryos were washed, incubated for 30 minutes in Ringer's solution at 28.5°C and fixed with 4% paraformaldehyde (PFA). When embryos were older than 2 days postfertilization (dpf), Ringer's solution with 10 mM BrdU was injected into the yolk of embryos. After at least a 2-hour incubation at 28.5°C, the embryos were fixed with 4% PFA.

Labelling for apoptosis

Embryos were fixed with 4% PFA and sectioned at 8 μm on a microtome cryostat, HM550M-OM (MICROM International GmbH). Apoptotic cells were detected by terminal deoxynucleotidyl transferase-mediated dUTP nick end labelling (TUNEL) using an in situ cell death detection kit (Roche).

DNA constructs for expressing dnPKA, p27, ΔN-Tcf3 and Δ47-β-catenin

The pCS2 vector (Rupp et al., 1994) carrying mouse dnPKA was described by Ungar and Moon (Ungar and Moon, 1996). This plasmid was modified to generate the expression construct pCS2[hsp:dnPKA], by replacing the CMV promoter with a zebrafish heat-shock inducible promoter (hsp) (Halloran et al., 2000). The coding region of *Xenopus* p27 (Su et al., 1995) and zebrafish ΔN-Tcf3 (Kim et al., 2000) was inserted into the pCS2MT expression vector, resulting in the addition of the myc-tag to the N terminus of these proteins. GFP was fused to the C terminus of the coding region of Δ47-β-catenin (Chenn and Walsh, 2002). These plasmids were modified to generate the expression constructs pCS2[hsp:myc-p27], pCS2[hsp:myc-ΔN-Tcf3] and pCS2[hsp:Δ47-β-catenin-GFP], by replacing the CMV promoter with zebrafish hsp.

Heat-shock treatment and BrdU labelling of embryos injected with the DNA construct

Embryos injected with the construct pCS2[hsp:dnPKA], pCS2[hsp:myc-p27] or pCS2[hsp:myc-ΔTcf3] were incubated at 39°C from 17 to 18 hpf, and soaked in water containing forskolin from 18 hpf. Embryos expressing dnPKA were fixed with 4% PFA at 33 hpf and examined for in situ hybridisation with the *ath5* RNA probe. At 33 hpf, embryos expressing p27 or ΔTcf3 were labelled with BrdU and then fixed with PFA at least 2 hours after the BrdU incorporation. These embryos were labelled with the anti-myc antibody and signals were visualised by staining with HRP-conjugated anti-mouse IgG antibodies (Histofine kit, Nichirei), using 3,3′-diaminobenzidine (DAB) (Sigma) as a substrate. These labelled embryos were sectioned using a cryostat and the cryosections were treated with 2N HCl for 60 minutes to expose the nuclei. After HCl treatment, sections were labelled with the anti-BrdU antibody and BrdU-positive areas were visualised as fluorescence by labelling with Alexa532-conjugated anti-mouse IgG antibody. HCl treatment seems to inactivate the epitope structures of the anti-myc antibody, resulting in an absence of cross-reactions between the Alexa532 anti-mouse IgG antibody and anti-myc antibody.

Co-expression of dnPKA and Δ47-β-catenin

A mixture of plasmids, pCS2[hsp:dnPKA] (30 μg/ml) and pCS2[hsp:Δ47-β-catenin-GFP] (30 μg/ml), was injected into embryos. Embryos were incubated at 39°C from 17 to 18 hpf, developed until 48 hpf and then fixed with 4% PFA.

Cloning of zebrafish homologues of the cdk inhibitor p27

We searched the zebrafish genomic database, which has been provided by the Wellcome Trust Sanger Institute, and identified two zebrafish homologues of p27. Their Ensembl gene identification numbers in this database are ENSDARG00000020832 and ENSDARG00000010878, which are referred to as p27a and p27b, respectively, hereafter. The sequences of p27a and p27b have been deposited in GenBank with the Accession numbers AF398516 and BI887574 (EST sequence), respectively. Their cDNA fragments were amplified by PCR using primers specific to their 5′ and 3′ sequences. The phylogenetic tree was constructed on the basis of the full-length amino acid sequences using the GENETYX-MAC program based on the Neighbour-Joining (NJ) method (Software Development).

Calculation of the ratio of BrdU-positive area to total area within the neural retina

Cryosections labelled with the anti-BrdU antibody were scanned under a LSM 510 laser-scanning microscope (Carl Zeiss). Using NIH Image, BrdU signals were converted to a binary scale with two digits, 0 (negative) and 1 (positive), by which the BrdU-positive area is adjusted to the outlines of BrdU-positive cells. This procedure approximates the ratio of the BrdU-positive area to the total area to the ratio of BrdU-positive cell number to total cell number. The number of pixels corresponding to 1 and 0 within the neural retina was determined. The ratio of the BrdU-positive area to the total area was calculated as the ratio of the number of 1 pixels to the number of 1+0 pixels.

Morpholino oligonucleotide injection

Morpholinos were purchased from Gene Tools. Anti-sense morpholino oligonucleotides for *shh* (shh-MO), *twhh* (twhh-MO), *Gli1* (Gli1-MO) and *Gli2* (Gli2-MO) genes were designed as previously described (Nasevicius and Ekker, 2000; Karlstrom et al., 2003). A mixture of shh-MO (1 mg/ml) and twhh-MO (1 mg/ml), or a mixture of Gli1-MO (1 mg/ml) and Gli2-MO (1 mg/ml), was injected into the yolk. Injected embryos were incubated until they

reached the appropriate stage and then fixed with 4% PFA for in situ hybridisation, plastic section or antibody labelling.

Assessment of severity of the progression of *ath5* expression in the blockade of Hh signalling

According to the severity of the defect in *ath5* expression, embryos labelled with *ath5* RNA probe were classified into four groups: no expression, severe, mild and normal. Severe means that *ath5* expression is initiated in the ventronasal retina but fails to spread to the dorsal and temporal retina. Mild means that the progression of *ath5* expression occurs to some degree but does not reach the whole of the neural retina. Typical examples are shown in Fig. 4L-L″.

Results

Forskolin treatment effectively blocks the progression of *ath5* expression and RGC differentiation

Our previous study showed that a zebrafish homologue of *Drosophila atonal*, *ath5*, is expressed transiently in retinoblasts undergoing the final mitosis and also in their postmitotic daughter cells (Masai et al., 2000) (Fig. 5D), indicating that *ath5* is the earliest marker of neuronal production. In zebrafish, *ath5* mRNA was expressed at the ventronasal retina at 25 hpf (Fig. 1A), and its expression spread to the dorsal and temporal regions in a fan-shaped manner at 27 hpf (Fig. 1B). This fan-shaped expression pattern spread from the central to peripheral regions in the later stages of development (31 hpf; Fig. 1C). The profile of *ath5* expression agrees with that of neuronal production shown by a previous study using BrdU incorporation (Hu and Easter, 1999). Another study demonstrated that the progression of *ath5* expression is inhibited in only 20% of embryos treated with the Hh inhibitor cyclopamine (Stenkamp and Frey, 2003), which is a teratogenic *Veratrum* alkaloid that inhibits the function of Smo (Cooper et al., 1998; Chen et al., 2002). Here, we used another chemical, forskolin, which directly stimulates adenylyl cyclase to increase cellular cAMP levels, constitutively activating PKA, which inhibits Hh signalling (Barresi et al., 2000; Ingham and McMahon, 2001; Cohen, 2003). Forskolin treatment did not affect the initiation of *ath5* expression in a few cells adjacent to the optic stalk, but it completely blocked the progression of *ath5* expression at 33 hpf (Fig. 1E). The penetrance of this phenotype induced by forskolin treatment was almost 100% (n>100 embryos). The introduction of a dominant-negative PKA (dnPKA) rescued the progression of *ath5* expression in forskolin-treated embryos (Fig. 1F), suggesting that the constitutive activation of PKA inhibits the progression of *ath5* expression. Together, these data suggest that the initial induction of *ath5* expression in the ventronasal retina is independent of PKA activity, and that a high level of PKA activity strongly inhibits the progression of *ath5* expression to the rest of the neural retina. We confirmed that treatment with cyclopamine caused only a mild delay of *ath5* expression (Fig. 1G,H), indicating that the effect of forskolin on *ath5* expression is more severe than that of cyclopamine.

As the removal of Ath5 function affects RGC differentiation (Kay et al., 2001), we examined whether forskolin treatment affects the differentiation of RGCs. In forskolin-treated retinas, the differentiation makers of RGCs *islet1* (Inoue et al., 1994) and *lim3* (Glasgow et al., 1997) were normally expressed in a few cells adjacent to the optic stalk, but the progression of their expression was completely blocked (100%, n=20, Fig. 1J; 100%, n=20, Fig. 1L). These data indicate that the progression of RGC differentiation is blocked

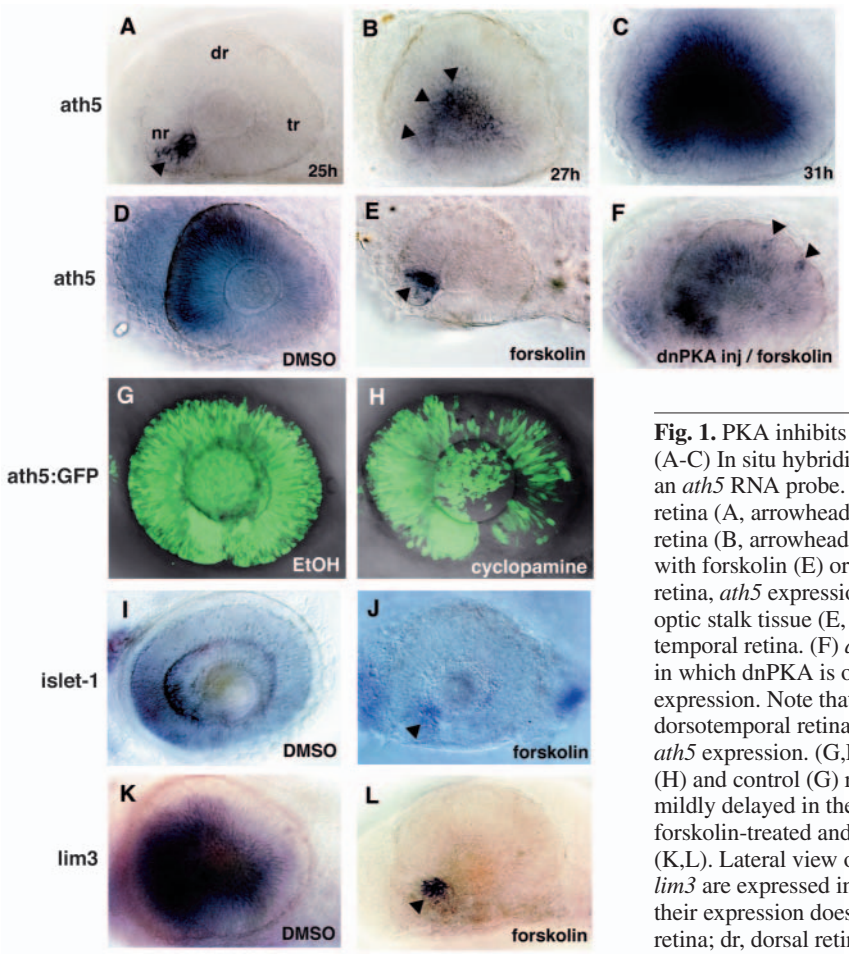

Fig. 1. PKA inhibits the wave of neurogenesis in the zebrafish retina. (A-C) In situ hybridisation of embryos at 25 (A), 27 (B) and 31 (C) hpf with an *ath5* RNA probe. *ath5* mRNA expression is initiated at the ventronasal retina (A, arrowhead) and progresses to the central region of the neural retina (B, arrowheads). (D,E) *ath5* expression in the 33-hpf retina treated with forskolin (E) or with DMSO as a control (D). In the forskolin-treated retina, *ath5* expression is initiated normally in a few cells adjacent to the optic stalk tissue (E, arrowhead), but does not spread to the dorsal and temporal retina. (F) *ath5* expression in the 33-hpf forskolin-treated embryo in which dnPKA is overexpressed. Overexpression of dnPKA rescues *ath5* expression. Note that *ath5* expression is observed in isolated cells in the dorsotemporal retina (arrowheads), suggesting cell-autonomous rescue of *ath5* expression. (G,H) ath5:GFP expression in 48-hpf cyclopamine-treated (H) and control (G) retinas. The progression of ath5:GFP expression is mildly delayed in the presence of cyclopamine. (I-L) In situ hybridisation of forskolin-treated and control retinas with *islet1* (I,J) and *lim3* RNA probes (K,L). Lateral view of optic cups at 48 (I,J) and 33 (K,L) hpf. Both *islet1* and *lim3* are expressed in a few cells adjacent to the optic stalk (arrowheads), but their expression does not progress in the presence of forskolin (J,L). nr, nasal retina; dr, dorsal retina; tr, temporal retina.

by the forskolin treatment. As *islet1/lim3*-positive RGCs are considered to be derived from *ath5*-positive cells treated with forskolin, forskolin does not simply inhibit neuronal differentiation but seems to block a process required for the progression of neuronal differentiation. We also examined the differentiation of other retinal cell-types such as photoreceptors in forskolin-treated retinas. However, treatment with forskolin or DMSO induced massive cell death after 48 hpf, which masked any phenotype of their differentiation (data not shown; see Fig. 2J). Thus, in this study, we focus upon the differentiation from retinoblasts to RGCs.

Forskolin treatment blocks cell-cycle exit of retinal progenitor cells

To examine whether forskolin-treated retinal cells are mitotic, we examined the markers of mitotic cells and BrdU incorporation. In 2-dpf wild-type retinas, *rx1* expression was downregulated in differentiating neurons and localised in the ciliary marginal zone (CMZ), which corresponds to the proliferating region (Chuang et al., 1999) (Fig. 2B). In forskolin-treated retinas, expression of *rx1* was not downregulated and it remained expressed throughout the neural retina (Fig. 2A). Forskolin-treated retinas were labelled with the anti-phosphorylated histone H3 antibody, which can label mitotic cells in the late G2 and M phases (Wei and Allis, 1998). In 2-dpf wild-type retinas, the nuclei of dividing cells were localised to the CMZ (Fig. 2D). In forskolin-treated retinas, dividing cells were still detected at the ventricular surface throughout the neural retina and they did not localise to the CMZ (Fig. 2C). We examined BrdU incorporation in forskolin-treated retinas. The ratio of BrdU-positive retinal cells was higher in forskolin-treated retinas than in control DMSO-treated retinas (Fig. 2E,F,I). These data suggest that a large population of retinal cells is mitotic in the presence of forskolin.

To exclude the possibility that postmitotic cells die immediately after their generation in the presence of forskolin, their cell death pattern was examined by labelling with Acridine Orange. Apoptosis was observed in both forskolin-treated and control DMSO-treated retinas but its spatiotemporal cell death pattern did not correlate with the pattern of progression of *ath5* expression (data not shown). Even though their cell death pattern does not correlate to the pattern of progression of *ath5* expression, forskolin treatment has an effect on the maintenance of retinal cells. TUNEL analysis of cryosections revealed that at 33 hpf the number of apoptotic cells in the presence of forskolin was more than three times higher than that in the presence of DMSO (Fig. 2G,H,J), suggesting that forskolin treatment affects the survival of mitotic retinal cells. From 33 to 48 hpf, the number of apoptotic cells increased not only in forskolin-treated retinas but also in DMSO-treated retinas (Fig. 2J), suggesting that retinal cells are sensitive to DMSO after 33 hpf.

PKA inhibits the exit of retinoblasts from Wnt-dependent cell-cycle progression

To elucidate whether PKA inhibits cell-cycle exit upstream of cyclin D1 and p27, we examined the expression of these genes in forskolin-treated retinas. To identify zebrafish p27 genes, we searched the zebrafish genome database and found that there are at least two p27 homologues in zebrafish, which are designated p27a and p27b (see Materials and methods). The phylogenetic relationship among the p27 family proteins

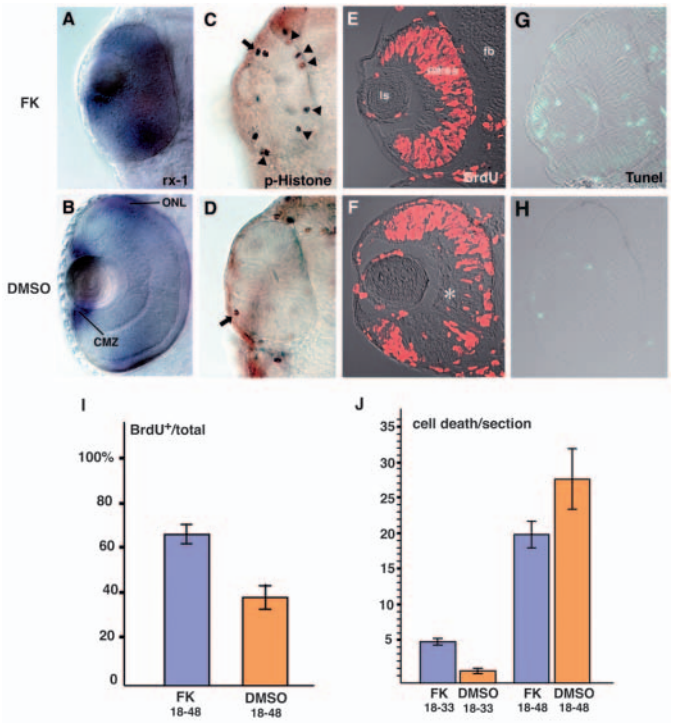

Fig. 2. PKA inhibits cell-cycle exit of retinal progenitor cells. (A,B) *rx1* expression in 48-hpf forskolin-treated (A) and DMSO-treated (B) retinas. *rx1* is expressed both in the outer nuclear layer (ONL) and in the CMZ of DMSO-treated retinas (B); expression is not downregulated in the presence of forskolin (A). (C,D) Labelling of 33-hpf retinas with anti-phosphorylated histone H3 antibody. In the forskolin-treated retina (C), antibody staining was observed in the CMZ (arrow) and at the ventricular surface of the neural retina (arrowheads), whereas only a few mitotic cells were observed in the CMZ (arrow) of the DMSO-treated retina (D). (E,F) BrdU labelling of 48-hpf forskolin-treated (E) and DMSO-treated (F) retinas. In the forskolin-treated retina, most of retinal cells are BrdU positive, whereas cell division seems to cease in the RGC and amacrine cell layers (asterisk) in the DMSO-treated retina. (G,H) TUNEL analysis of 33-hpf forskolin-treated (G) and DMSO-treated (H) retinas. Patterns of cell apoptosis (green) do not correlate with those of neuronal production in forskolin-treated retinas (G; data not shown), although the number of apoptotic cells is higher than in DMSO-treated retinas (H). (I) Ratios of BrdU-positive areas to total area in forskolin- and DMSO-treated retinas. Bars indicate the average ratios that were observed in cryosections of the retinas labelled with the anti-BrdU antibody. The numbers of embryos examined were n=3 and n=2 for forskolin treatment (FK 18-48) and DMSO treatment (DMSO 18-48) between 18 and 48 hpf, respectively. Four sections from the nasal to temporal regions were examined per embryo. (J) Quantification of apoptotic cells in forskolin- and DMSO-treated retinas. Bars indicate the average number of apoptotic cells observed in cryosections corresponding to the central retina subjected to TUNEL. One section was examined per embryo. The numbers of embryos examined were n=7 for forskolin treatment between 18 and 33 hpf (FK 18-33), n=3 for DMSO treatment between 18 and 33 hpf (DMSO 18-33), n=5 for forskolin between 18 and 48 hpf (FK 18-48), and n=3 for DMSO treatment between 18 and 48 hpf (DMSO 18-48). CMZ, ciliary marginal zone; fb, forebrain; FK, forskolin; ls, lens; ONL, outer nuclear layer.

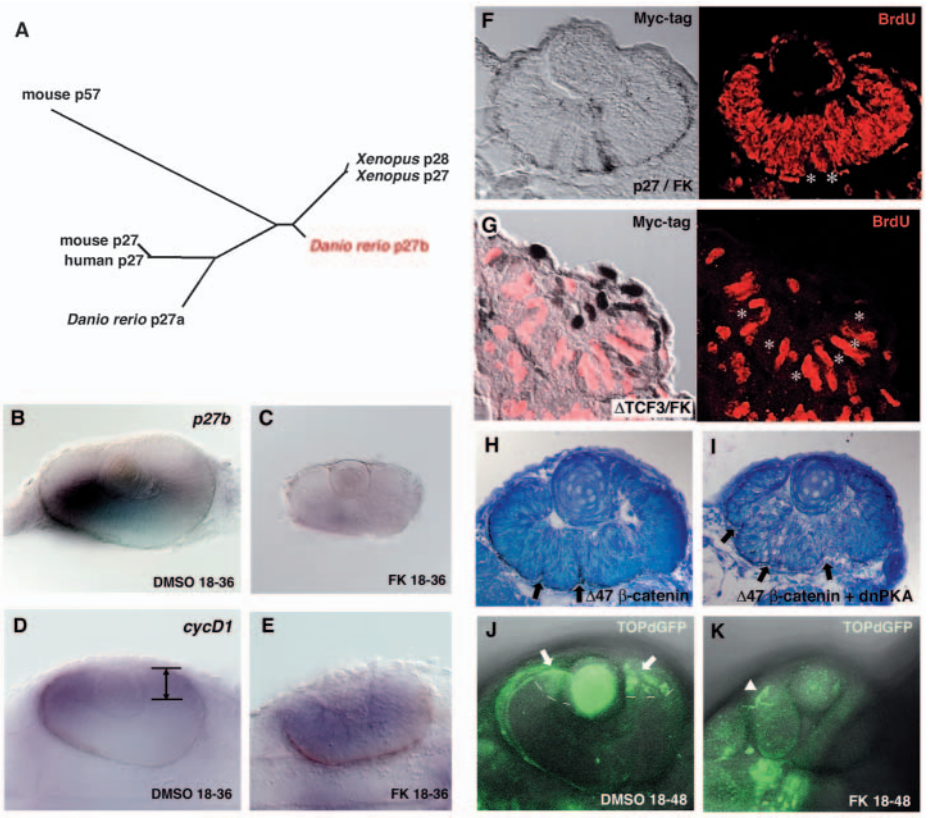

Fig. 3. Canonical Wnt signalling is required for PKA-mediated cell proliferation. (A) Phylogenetic relationship among vertebrate p27 proteins and mouse p57. The length of each branch is proportional to sequence divergence from the branch points. (B,C) In situ hybridisation of 36-hpf DMSO- and forskolin-treated retinas with a *p27b* RNA probe. *p27b* is expressed in the DMSO-treated retina (B) but not in the forskolin-treated retina (C). (D,E) In situ hybridisation of 36-hpf DMSO-treated (D) and forskolin-treated (E) retinas with a *cyclin D1* RNA probe. *cyclin D1* is downregulated in differentiating neurons and is localised in the CMZ of the DMSO-treated retina (D, lines/arrows). However, *cyclin D1* is not downregulated in the forskolin-treated retina (E) but remains expressed in a large region. (F) 48-hpf forskolin-treated embryos expressing myc-tagged p27 labelled with the anti-myc antibody (brown in left panel) and anti-BrdU antibody (red in right panel). Retinal cells expressing p27 are BrdU negative (white asterisks), whereas almost all p27-negative cells incorporate BrdU. (G) 33-hpf forskolin-treated embryos expressing myc-tagged ΔN-Tcf3 labelled with the anti-myc antibody (brown in left panel) and anti-BrdU antibody (red). Retinal cells expressing ΔN-Tcf3 are BrdU negative (white asterisks). (H,I) 48-hpf wild-type retinas expressing Δ47-β-catenin (H) and a mixture of Δ47-β-catenin and dnPKA (I). Multi-folded neural retina is observed (arrows) in both cases, suggesting that dnPKA does not inhibit Wnt-induced proliferation. (J,K) GFP expression in 2-dpf TOPdGFP transgenic retinas treated with DMSO (J) and forskolin (K). GFP is expressed in the CMZ of the DMSO-treated retina (J, arrows and white dashed lines). In the forskolin-treated retina, GFP expression is not detected. Arrowhead (K) indicates GFP expression in epidermis.

revealed that p27a is similar to mouse and human p27, whereas p27b is more similar to *Xenopus* p27 (Fig. 3A). In situ hybridisation analysis revealed that *p27b* is expressed in the zebrafish retina, whereas *p27a* is expressed in the lens rather than in the neural retina (data not shown). *p27b* expression was probably localised in mitotic retinoblasts and early differentiating neurons (Fig. 3B; data not shown). *p27b* expression was markedly weak or absent in forskolin-treated retinas (Fig. 3C). The expression of *cyclin D1* was downregulated in differentiating neurons and localised in the CMZ in wild-type retinas (Fig. 3D). However, *cyclin D1* expression was not downregulated and remained in a large area of the forskolin-treated retina (Fig. 3E). We examined the transcription level of *cyclin D1* by the quantitative PCR analysis and found that the transcription level of *cyclin D1* is relatively normal in forskolin-treated heads (data not shown), suggesting that the aberrant increase in *cyclin D1* expression does not occur in the forskolin-treated retina. Furthermore, ectopic introduction of *Xenopus* p27 inhibited cell-cycle progression in the forskolin-treated retina (Fig. 3F; 100%, n=15 retinal columns), although almost all p27 non-expressing cells were BrdU-positive. These data suggest that PKA inhibits the cell-cycle exit of retinal cells upstream of the interaction between cyclin D1 and p27.

Cyclin D1 is a direct target of Wnt/β-catenin signalling (Tetsu and McCormick, 1999). It was reported that canonical Wnt signalling promotes cell proliferation in chick retinas (Kubo et al., 2003). Recently, we also found that Wnt/β-catenin signalling is activated in proliferating cells in the zebrafish retina, and that the activation of canonical Wnt signalling induces hyperproliferation in the zebrafish retina (M.Y. and I.M., unpublished). To elucidate whether Wnt/β-catenin signalling is required for PKA-mediated proliferation, we examined BrdU incorporation in forskolin-treated retinas with overexpressed ΔN-Tcf3, a deletion of T cell factor 3 (Tcf3) that lacks β-catenin binding and functions as a dominant suppressor of Wnt signalling (Kim et al., 2000). Retinal cells expressing ΔN-Tcf3 did not incorporate BrdU even in the presence of forskolin (Fig. 3G; 100%, n=92). These data suggest that Wnt signalling is required for PKA-mediated proliferation.

Recently, we found that proliferation is enhanced in the zebrafish retina by the introduction of Δ47-β-catenin, which lacks N-terminal phosphorylation sites and functions as a constitutively active form of β-catenin (Chenn and Walsh, 2002) (M.Y. and I.M., unpublished) (Fig. 3H). To elucidate whether PKA activity is required for Wnt-mediated proliferation, we examined retinal phenotypes of embryos injected with a mixture of Δ47-β-catenin and dnPKA. The introduction of dnPKA did not suppress the hyperproliferation induced by Δ47-β-catenin (Fig. 3I), suggesting that a high level of Wnt activity can overcome the loss of PKA activity to promote proliferation. These data suggest that Wnt signalling is epistatic to PKA in the proliferation of retinal cells.

To elucidate whether Wnt signalling is activated by PKA,

we used TOPdGFP transgenic fish carrying GFP under the control of a β-catenin responsive promoter (Dorsky et al., 2002). In TOPdGFP fish, GFP is expressed in the CMZ at 2 dpf (Fig. 3J), suggesting that the activation of Wnt signalling occurs in proliferating retinal cells. Forskolin treatment did not enhance this GFP expression in the neural retina (Fig. 3K), suggesting that PKA does not activate the Wnt signalling pathway. Together, these data suggest that PKA inhibits exit from the Wnt-mediated cell cycle, rather than stimulating cell-cycle progression through the activation of Wnt signalling.

The cell-cycle exit of retinal mitotic cells is affected in the blockade of Smo and Gli functions

A previous study demonstrated that the induction and progression of *ath5* expression are variably perturbed in the zebrafish *smo* mutant *slow-muscle-omitted* (*smu*) (Stenkamp

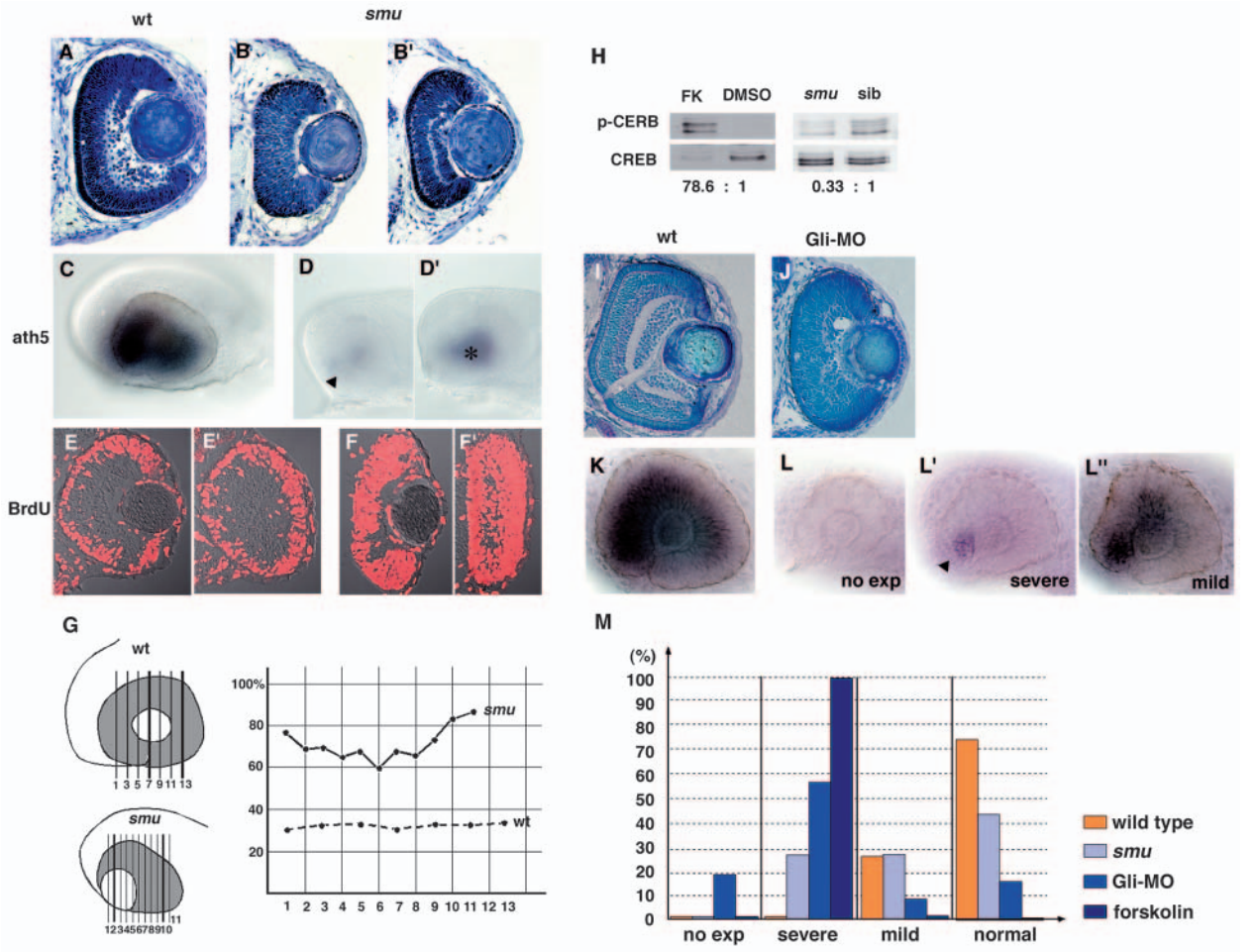

Fig. 4. The wave of retinal neurogenesis is affected in *smu* mutant and Gli-MO-injected embryos. (A-B′) Plastic sectioning of wild-type (A) and *smu*$^{b577-/-}$ (B,B′) retinas at 48 hpf. In *smu*$^{b577-/-}$ retinas, lamination defects vary. No lamination is observed in the most severe phenotype (B) and a nearly normal lamination occurs in the mildest phenotype (B′). (C-D′) *ath5* expression in wild-type (C) and *smu*$^{b577-/-}$ (D,D′) retinas at 33 hpf. *ath5* expression is initiated at the ventro-nasal retina (D, arrowhead) but does not spread to the entire eyes in *smu*$^{b577-/-}$ embryos. This phenotype varies from severe (D) to mild (D′, asterisk), and the defect in *ath5* expression is proportional to that of a cyclopic phenotype. (E-F′) Labelling of 48-hpf wild-type (E,E′) and *smu*$^{b577-/-}$(F,F′) retinas with the anti-BrdU antibody. (E,F) Central retinas of wild-type (E) and *smu*$^{b577-/-}$ embryos (F). These sections correspond to no.7 (wild-type) and no.2 (*smu*$^{-/-}$) shown in G, respectively. (E′,F′) Peripheral retinas of wild-type (E′) and *smu*$^{b577-/-}$ (F′) embryos. These sections correspond to no.13 (wild-type) and no.10 (*smu*$^{-/-}$) shown in G, respectively. (G) Spatial profile of the ratio of BrdU-positive area to total area in wild-type and *smu*$^{b577-/-}$ retinas. Solid and dotted lines indicate *smu*$^{-/-}$ and wild-type sibling retinas, respectively. Numbers represent anterior-posterior locations of cryosections, which are shown in the left schematic drawing. (H) Western blot analysis of forskolin-treated and *smu*$^{b577-/-}$ heads using antibodies against Ser133-phosphorylated CREB (upper) and CREB (lower). The phosphorylation of CREB is more than 70 times higher in forskolin-treated heads than in control DMSO-treated heads. However, in *smu*$^{b577-/-}$ heads, CREB phosphorylation is decreased to one-third of the normal level. (I,J) Plastic sectioning of wild-type (I) and Gli-MO-injected (J) retinas at 3 dpf. In the severe case of Gli-MO-injected embryos, retinal lamination is severely delayed. (K-L″) In situ hybridisation of 33-hpf wild-type (K) and Gli-MO-injected (L-L″) embryos with an *ath5* RNA probe. The progression of *ath5* expression is perturbed to different degrees in Gli-MO-injected retinas, from no initiation (L), to severe (L′) or mild (L″) inhibition. In the severe case, *ath5* expression is only observed in the ventronasal retina (L′, arrowhead). (M) Quantitative assessment of *ath5* expression in wild-type (orange), *smu* mutant (light blue), Gli-MO-injected (blue) and forskolin-treated (dark blue) embryos. Embryos were classified into four groups according to the severity of the defect in *ath5* expression, as shown in (L-L″) and counted in number. Numbers of examined embryos were n=11 for wild type, n=21 for the *smu* mutant, n=63 for Gli-MO-injected embryos and n>100 for forskolin-treated embryos. Almost all of the forskolin-treated embryos show the 'severe' phenotype. FK, forskolin.

and Frey, 2003). Here, we show that the cell-cycle exit of retinal progenitor cells is perturbed in *smu* mutants. In *smu*$^{b577-/-}$ retinas, lamination was usually delayed (Fig. 4B,B′). In the *smu*^{b577} mutant, the initial induction of *ath5* expression occurred in the presumptive ventronasal retina, but the progression of *ath5* expression was variably affected among *smu*$^{b577-/-}$ embryos from severe (*n*=6/21, Fig. 4D) to mild (*n*=6/21, Fig. 4D′). The delay of *ath5* expression became less severe in the *smu*^{b577} mutant in later stages, and *ath5* expression occurred in a large region of the neural retina until 3 dpf (data not shown). In 2-dpf wild-type retinas, the anti-BrdU antibody strongly labelled retinal cells in the CMZ and the outer layer, but not in the RGC and inner layers, where the majority of neuronal cells were born until 2 dpf (Fig. 4E,E′). The ratio of BrdU-positive cells relative to the total number of cells was about 30% on average in wild-type retinas, which remained constant from the nasal to temporal regions within the optic cup (Fig. 4G). In the severe cases of *smu*^{b577} mutants, a large number of retinal cells were BrdU-positive (Figs. 4F,F′). On average, 70% of cells were BrdU positive in severe cases, more than twice that in wild-type embryos. BrdU labelling of serial sections of the *smu*$^{b577-/-}$ retina revealed that more than 80% of cells in the temporal region were mitotic, with the highest ratio of mitotic cells being found in the nasal-temporal axis (Fig. 4G). Since the wave of neuronal production spreads from the nasal to temporal retina, the high ratio in the temporal retina suggests that the progression of neuronal production is delayed in *smu*$^{b577-/-}$ retinas.

The progression of retinal neurogenesis is more severely inhibited in embryos treated with forskolin than in the *smu* mutant. The difference between forskolin treatment and the genetic blockade of Smo function might be the level of PKA activity. One of the major substrates of PKA is the cAMP-responsible element binding factor (CREB) (Lonze and Ginty, 2002). Because PKA phosphorylates Ser133 of CREB, we examined the level of this phosphorylation in forskolin-treated and *smu* mutant embryos. Western blot analysis with an antibody against phosphorylated Ser133 of CREB revealed that the level of CREB phosphorylation is much higher in forskolin-treated embryos than in control DMSO-treated embryos (Fig. 4H). By contrast, the level of CREB phosphorylation was not elevated in *smu* mutants (Fig. 4H). These data suggest that high activation of PKA occurs only after forskolin treatment.

As PKA inhibits the Hh signalling pathway by generating the repressor form of Gli, the repressor activity of Gli may be higher in the presence of forskolin than when Smo function is blocked. If this is the case, the level of the Gli repressor activity may correlate with the severity of the defect in retinal neurogenesis. An alternative possibility is that PKA activates Hh-independent signalling pathways, such as CREB, which might contribute to the forskolin-induced phenotype. To distinguish between these possibilities, we examined retinal phenotypes caused by the inhibition of Gli proteins, which function downstream of PKA. To inhibit Gli function, embryos were injected with a mixture of morpholino antisense oligonucleotides of Gli1 and Gli2 (Gli-MO). In Gli-MO-injected embryos, retinal lamination was severely delayed, as in the *smu* mutant (Fig. 4I,J). In Gli-MO-injected retinas, the progression of *ath5* expression was variably perturbed from no expression (*n*=12/63, Fig. 4L) to severe (*n*=36/63, Fig. 4L′), mild (*n*=5/63, Fig. 4L″) and almost normal (*n*=10/63, data not shown) expression. The severity of the progression defect in Gli-MO-injected embryos is intermediate between that observed in forskolin-treated embryos and that seen in *smu* mutant embryos (Fig. 4M). These data suggest that the blockade of Gli functions causes defects in the cell-cycle exit of retinal progenitor cells. Together, these data suggest that PKA inhibits Hh-mediated Gli activation, which regulates the progression of neuronal production.

A wave of *ath5* expression spreads to the temporal retina earlier than that of *shh:GFP* expression

Zebrafish Shh and Twhh are expressed in RGCs and induce RGC differentiation in neighbouring uncommitted areas (Neumann and Nuesslein-Volhard, 2000), raising the possibility that Hh produced by RGCs promotes mitotic retinoblasts to generate neurons. If this is the case, the progression of *ath5* expression must spatially and temporally correlate with that of RGC differentiation. However, several contradictory observations have been reported. Because the first RGCs start to extend their axons at 28 hpf (Laessing and Stuermer, 1996; Schmitt and Dowling, 1996), there is at least a 3-4 hour time lag between *ath5* expression and this first morphological appearance of RGC differentiation. Furthermore, cyclopamine treatment after 26 hpf completely inhibits the progression of RGC differentiation (Neumann and Neusslein-Volhard, 2000), although the progression of *ath5* expression is only mildly delayed by treatment with cyclopamine after 27 hpf (Stenkamp and Frey, 2003). These observations suggest that the progression of *ath5* expression does not strongly correlate with that of RGC differentiation. To elucidate why this lack of correlation occurs, we examined *ath5* and *shh* expression in more detail. *shh* expression was monitored by GFP expression under the control of *shh* retinal enhancers (referred to as shh:GFP). shh:GFP was expressed in the ventral forebrain only, and was not in the eye until at least 27 hpf (data not shown). shh:GFP expression was detected in a few cells in the ventronasal retina adjacent to the optic stalk at 29 hpf (Fig. 5A). Faint expression of shh:GFP progressed to the dorso-nasal retina at 31 hpf (Fig. 5B). shh:GFP expression spread to the temporal retina at 35 hpf (Fig. 5C). This expression profile is consistent with previous published data (Neumann and Nuesslein-Volhard, 2000), and suggests that shh:GFP expression correlates with the maturation of RGCs.

To facilitate the detection of *ath5* expression with high sensitivity, we used the transgenic line Tg(ath5:GFP) (Masai et al., 2003). BrdU labelling of retinas expressing ath5:GFP showed that ath5:GFP-expressing cells were BrdU-negative, suggesting that ath5:GFP is a marker of newly-generated postmitotic cells (Fig. 5D). Similar to the results of in situ hybridisation, ath5:GFP expression started in the ventronasal retina at 25 hpf (Fig. 5E). Compared with in situ hybridisation, it was more clearly demonstrated that the wave front of *ath5* expression had already reached the temporal retina at 27 hpf, although the density of GFP-positive cells was low (Fig. 5F). At 31 hpf, the area where ath5:GFP-positive cells were located became slightly larger and the number of ath5:GFP-positive cells increased (Fig. 5G). These data suggest that the wave of ath5:GFP expression progresses earlier than that of shh:GFP expression. To exclude the possibility that the time lag between ath5:GFP and shh:GFP is due to the difference of transgenic strains, we confirmed that *ath5* mRNA expression spreads to

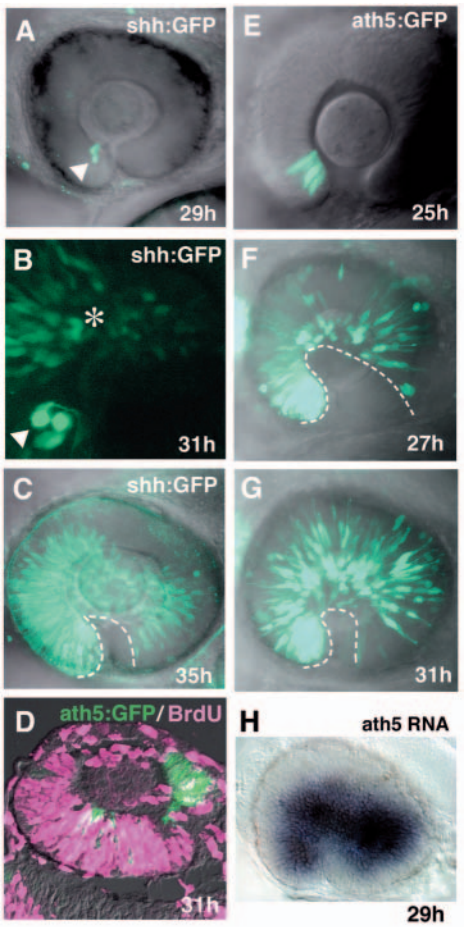

Fig. 5. Pattern of progression of shh:GFP and ath5:GFP expression in zebrafish retina. (A-C) Lateral view of the optic cup of the transgenic line Tg(shh:GFP). B is shown at twice the magnification of A and C. shh:GFP is expressed in a few cells adjacent to the optic stalk at 29 hpf (A, white arrowhead). Progression of GFP expression is observed in the adjacent dorsal region at 31 hpf (B, asterisk). A wave front of shh:GFP expression reaches the temporal region of the neural retina at 35 hpf (C, dotted line). (D) Double labelling of 31-hpf retinas of the transgenic line Tg(ath5:GFP) with the anti-BrdU antibody and ath5:GFP antibody. ath5:GFP-positive cells (green) are BrdU (magenta) negative. (E-G) GFP expression in the transgenic line Tg(ath5:GFP). Throughout the stages examined, the pattern of ath5:GFP expression is similar to that of *ath5* transcription. Note that GFP-expressing cells are already observed in the temporal region at 27 hpf (F), and the density of GFP-positive cells increases in later stages (G). The dotted line indicates a wave front of ath5:GFP expression. (H) *ath5* RNA expression in the transgenic line Tg(shh:GFP) at 29 hpf. This is the same embryo that is shown in A. *ath5* expression spreads to the large region of the neural retina.

the temporal retina at 29 hpf in shh:GFP transgenic embryos (Fig. 5H).

Forskolin treatment inhibits two distinct steps for RGC differentiation

The profile of *ath5*:GFP expression suggests that Hh signalling present before 27 hpf regulates the progression of neuronal production. To determine the critical period when Hh signalling is required for the progression of *ath5* expression, forskolin was applied within different time windows (Fig. 6M). To estimate the time lag from the forskolin treatment to the inhibition of Hh signalling pathway, we monitored *ptc1* expression during and after the forskolin pulse treatment. The expression of *ptc1* is regulated by Hh signalling and occurs in the ventral part of CNS at 24 hpf (Fig. 6A) (Concordet et al., 1996). Two hours after the start of forskolin treatment, *ptc1* expression severely decreased (n=5/5, Fig. 6B), suggesting that Hh signalling is suppressed within 2 hours of forskolin treatment (Fig. 6E). Two hours after the removal of forskolin, *ptc1* expression remained downregulated (n=6/6, Fig. 6C). By 4 hours after the removal of forskolin, *ptc1* expression had increased but was not fully recovered (data not shown). By 6 hours after the removal of forskolin, *ptc1* expression levels had recovered to the levels seen in control DMSO-treated embryos (n=6/6, Fig. 6D). These data suggest that Hh signalling is recovered between 2 and 6 hours after the removal of forskolin (Fig. 6E).

Here we monitored ath5:GFP and shh:GFP as markers of newly generated neurons and mature RGCs, respectively. Forskolin treatment before 22 hpf had no effect on the progression of ath5:GFP expression (Fig. 6F). Treatment from 18 to 24 hpf induced various phenotypes of ath5:GFP expression (Fig. 6G-G″), suggesting that forskolin treatment around 24 hpf inhibits the progression of ath5:GFP expression. Indeed, forskolin treatment between 22 and 26 hpf completely inhibited the progression of ath5:GFP expression (Fig. 6H). Interestingly, forskolin treatment after 27 hpf failed to block the progression of ath5:GFP expression (Fig. 6J) but completely inhibited the progression of the expression of shh:GFP (Fig. 6K) and that of another RGC marker, *islet1* (data not shown). To exclude the possibility that it is the difference in the transgenic strains that causes a different response to forskolin treatment between ath5:GFP and shh:GFP expression, we confirmed that *ath5* mRNA spreads to the large region of the neural retina in the Tg(shh:GFP) embryo shown in Fig. 6K (Fig. 6L). Together, these data suggest that Hh signalling regulates two distinct steps of RGC differentiation: cell-cycle exit of retinoblasts and the progression of *ath5*-positive immature neurons to mature RGCs. Considering the time lag between forskolin treatment and inhibition of the Hh signalling pathway (Fig. 6N), Hh signalling must regulate the progression of *ath5* expression between 24 and 29 hpf. Hh signalling after 29 hpf is not essential for the progression of *ath5* expression but is still required for the progression of RGC maturation.

Morpholino-antisense oligonucleotides for *shh* and *twhh* inhibits the wave of neuronal production

Pulse treatment with forskolin suggests that the wave of *ath5* expression is regulated by Hh activity that is present before 29 hpf. shh:GFP expression is initiated at 29 hpf (Fig. 5A). It was reported that *shh* RNA starts to be expressed at 28 hpf (Neumann and Nuesslein-Volhard, 2000). These observations raise the possibility that there is a very weak expression of *shh* and *twhh* in 24- to 29-hpf retinas, which is sufficient to regulate the wave of *ath5* expression. Alternatively, it is possible that Hh proteins other than Shh and Twhh regulate the progression of *ath5* expression. A third possibility is that *ath5* expression is not regulated by the short-range action of Hh signalling within the neural retina, but by the long-range action of Hh expressed in other tissues.

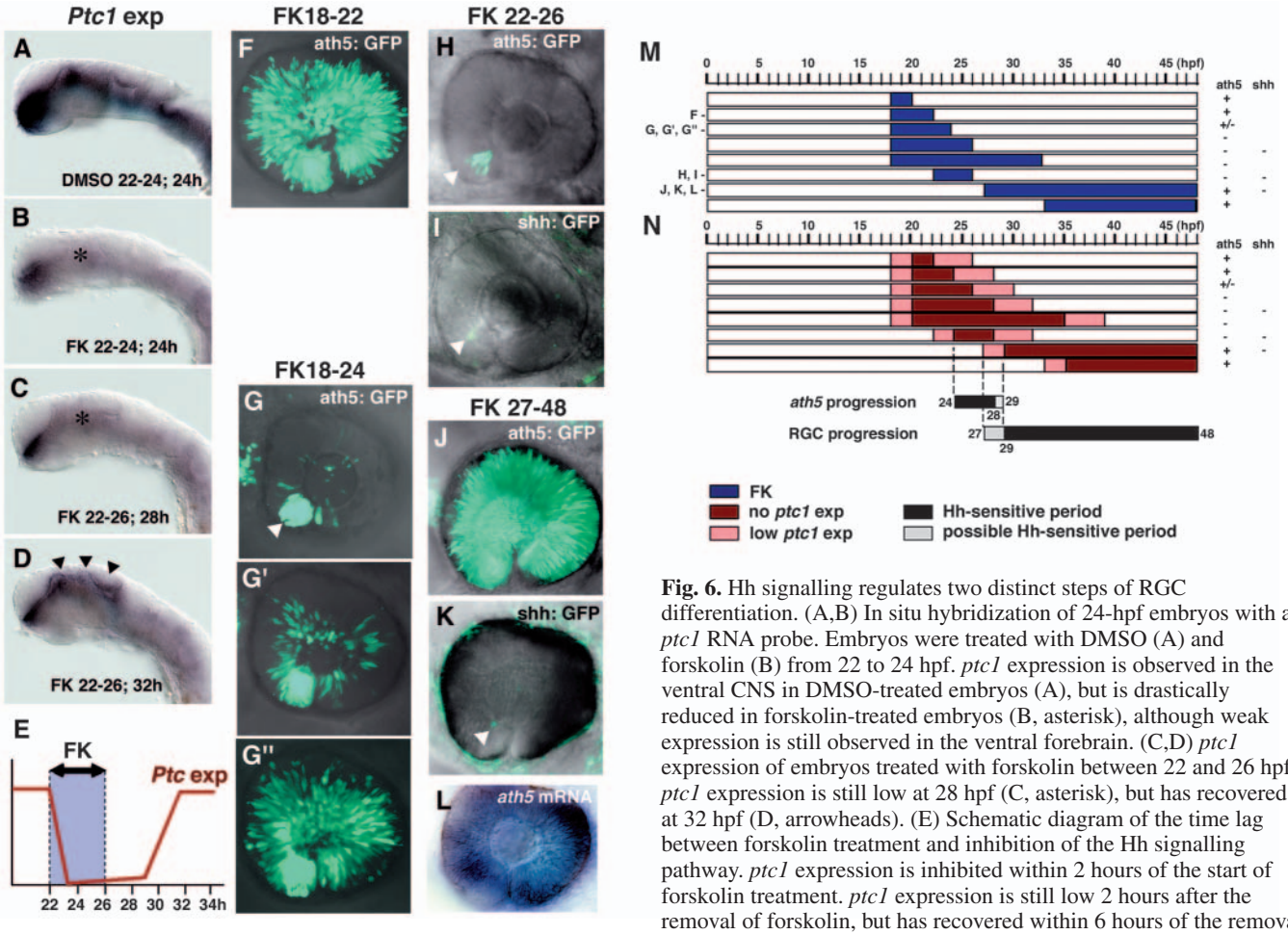

Fig. 6. Hh signalling regulates two distinct steps of RGC differentiation. (A,B) In situ hybridization of 24-hpf embryos with a *ptc1* RNA probe. Embryos were treated with DMSO (A) and forskolin (B) from 22 to 24 hpf. *ptc1* expression is observed in the ventral CNS in DMSO-treated embryos (A), but is drastically reduced in forskolin-treated embryos (B, asterisk), although weak expression is still observed in the ventral forebrain. (C,D) *ptc1* expression of embryos treated with forskolin between 22 and 26 hpf. *ptc1* expression is still low at 28 hpf (C, asterisk), but has recovered at 32 hpf (D, arrowheads). (E) Schematic diagram of the time lag between forskolin treatment and inhibition of the Hh signalling pathway. *ptc1* expression is inhibited within 2 hours of the start of forskolin treatment. *ptc1* expression is still low 2 hours after the removal of forskolin, but has recovered within 6 hours of the removal of forskolin. (F) ath5:GFP expression in retina treated with forskolin from 18 to 22 hpf; ath5:GFP expression progresses throughout the neural retina. (G-G″) ath5:GFP expression in retinas treated with forskolin from 18 to 24 hpf. The inhibition of progression varies from severe (G), to mild (G′) and nearly normal (G″). In the severe case, ath5:GFP is observed only in the ventronasal retina (white arrowhead). (H) ath5:GFP expression in retina treated with forskolin from 22 to 26 hpf. The progression of ath5:GFP expression is completely blocked (white arrowhead). (I) shh:GFP expression in retina treated with forskolin from 22 to 26 hpf. shh:GFP expression also fails to progress from the ventronasal retina (white arrowhead). (J) ath5:GFP expression in retina treated with forskolin from 27 to 48 hpf. The propagation of ath5:GFP expression occurs normally throughout the neural retina. (K) shh:GFP expression in retina treated with forskolin from 27 to 48 hpf. The progression of shh:GFP expression remains blocked (white arrowhead). Weak background signals are observed in the skin surrounding the eye. (L) *ath5* RNA expression in the same embryo as shown in K. *ath5* RNA expression spreads to whole region of the neural retina. (M) Pulse treatment with forskolin in different time windows. Blue bars indicate the period of treatment with forskolin. All embryos were examined at 48 hpf. +, progression of ath5:GFP or shh:GFP expression occurs normally; – indicates that progression is effectively blocked. (N) Time-window of Hh signalling inhibition, estimated by considering the time lag between forskolin treatment and the downregulation of *ptc1* expression. Red bars indicate the period when *ptc1* expression is severely suppressed by forskolin treatment. Pink bars indicate the time lag between the start of forskolin treatment and the suppression of *ptc1* expression, or between the removal of forskolin and the recovery of *ptc1* expression; within these time periods Hh signalling may be reduced. Black and grey bars indicate Hh-sensitive and possible Hh-sensitive periods for the progression of *ath5* expression and RGC maturation, respectively. FK, forskolin.

To investigate whether inhibition of the Shh- and Twhh-mediated pathway has an effect on the progression of *ath5* expression, we examined the phenotypes of embryos injected with a mixture of morpholino-antisense oligonucleotides for Shh and Twhh (hh-MO). In hh-MO-injected retinas, the progression of *ath5* and *islet1* expression was perturbed (Fig. 7B,D). Retinal cells in hh-MO-injected embryos largely incorporated BrdU (Fig. 7F). The severity of the defect in *ath5* expression in hh-MO-injected embryos was similar to that in Gli-MO-injected embryos (Fig. 7G, compare with Fig. 4M), suggesting that Shh and Twhh regulates the progression of *ath5* expression. To elucidate whether the local depletion of Shh and Twhh activities within the neural retina affects *ath5* expression, hh-MO-injected donor cells were transplanted into wild-type host retinas. In this experiment, to facilitate the detection of *ath5* expression, we used the transgenic line Tg(ath5:GFP). ath5:GFP expression was rarely observed in retinal cells derived from hh-MO-injected donor cells (Fig. 7H,I; n=5/5 embryos), and in some cases, ath5:GFP was not detected in wild-type cells located adjacent to the temporal side of hh-MO-injected cells (Fig. 7J), suggesting that Hh activity in the neural retina is necessary to regulate the progression of *ath5*

expression. Taken together, these data suggest that short-range Shh and Twhh signalling regulates the wave of neuronal production in the zebrafish retina.

Discussion

In this paper, we show that the progression of neuronal production in the zebrafish retina is completely inhibited by the activation of PKA, which negatively regulates Hh signalling. The blockade of Hh signalling molecules, including Hh, Smo and Gli, induces similar defects in the wave of neuronal production. These data suggest that Hh signalling regulates the progression of neuronal production in the zebrafish retina. In the presence of forskolin, one or two postmitotic neurons are generated adjacent to the optic stalk. This observation indicates that the initial induction of retinal neurogenesis is independent of PKA and is tightly localised in one or two cells located adjacent to the optic stalk, supporting the idea that signals from the optic stalk regulate the initial induction of neuronal production (Masai et al., 2000). A previous study reported that Shh is expressed in mature RGCs and acts on neighbouring undifferentiated cells to induce RGC differentiation (Neumann and Nuesslein-Volhard, 2000), raising the possibility that Shh expressed in RGCs induces neighbouring mitotic progenitor cells to exit from the cell cycle. However, we show that Hh signalling regulates two distinct steps of RGC differentiation: the cell-cycle exit of retinoblasts and RGC maturation. This dual requirement of Hh signalling in RGC differentiation suggests that the mechanism underlying the neurogenic wave in the zebrafish retina is more complex than that in the *Drosophila* compound eye.

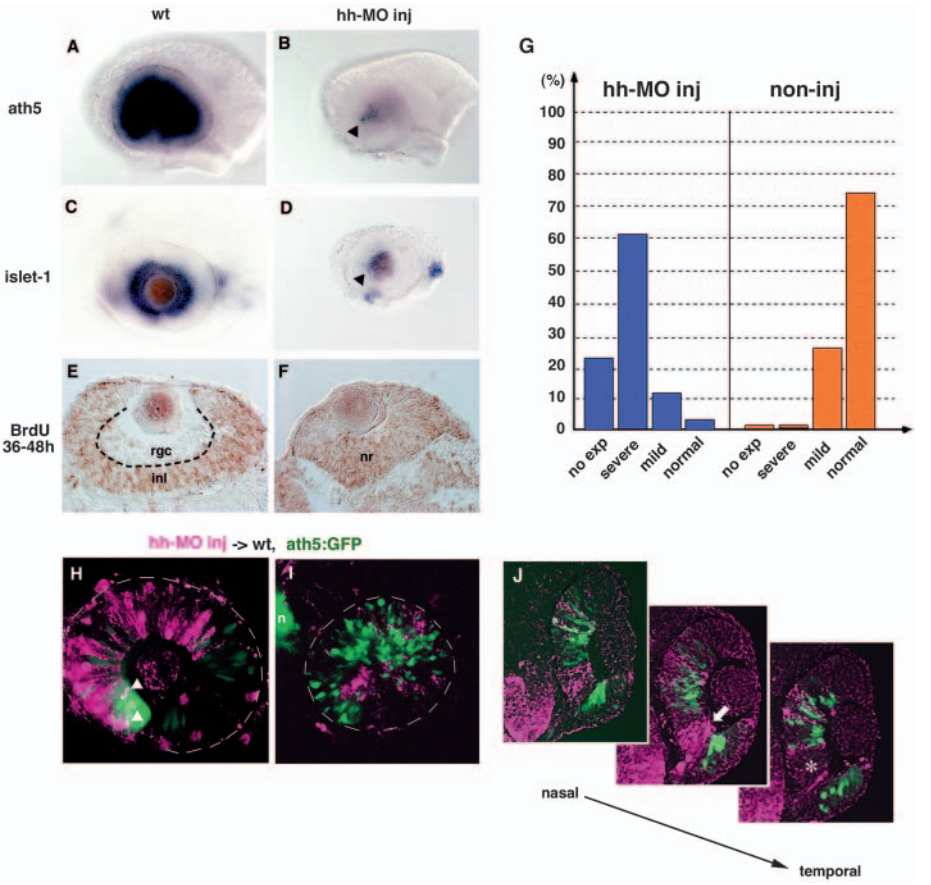

Fig. 7. Shh and Twhh regulate the progression of *ath5* expression. (A,B) *ath5* expression in 33-hpf wild-type (A) and Hh-MO-injected (B) retinas. *ath5* expression fails to progress from the ventronasal retina injected with Hh-MO (arrowhead). (C,D) *islet1* expression in 48-hpf wild-type (C) and Hh-MO-injected (D) retinas. *islet1* expression fails to progress from the ventronasal retina injected with Hh-MO (arrowhead). (E,F) Labelling of 48-hpf wild-type (E) and Hh-MO injected (F) retinas with an anti-BrdU antibody (brown). Because BrdU is incorporated from 36 to 48 hpf, the RGC layer is BrdU negative in the wild-type retina. By contrast, almost all retinal cells are labelled with the anti-BrdU antibody in the Hh-MO-injected retina. (G) Quantitative assessment of *ath5* expression in Hh-MO-injected (blue) and non-injected control (orange) embryos. The defect in *ath5* expression in Hh-MO-injected embryos shows a similar profile to that in Gli-MO-injected embryos (blue bars in Fig. 4M). Numbers of Hh-MO-injected and non-injected embryos examined were 33 and 11, respectively. (H) Hh-MO-injected cells were incorporated into 36-hpf wild-type peripheral retina. ath5:GFP expression (green) does not progress towards the Hh-MO-positive area (magenta), although double-positive cells (white arrowheads) are observed at the interface between wild-type and Hh-MO areas. (I) Hh-MO-injected cells were incorporated into 36 hpf wild-type central retina. Hh-MO (magenta) and ath5:GFP (green) are segregated. (J) Three adjacent sections are shown along the axis from the nasal to temporal regions. ath5:GFP expression (green) does not occur in retinal columns derived from Hh-MO-injected donor embryos (magenta). GFP is not expressed even in wild-type retinal columns (white asterisk in right panel) located adjacent to the temporal side of Hh-MO-derived retinal columns (white arrow in middle panel). inl, inner nuclear layer; n, nose; nr, neural retina; rgc, retinal ganglion cell layer.

PKA inhibits cell-cycle exit of retinoblasts through interaction with both Hh and Wnt signalling

In the presence of forskolin, *cyclin D1* expression is not downregulated and *p27* expression severely decreases. Furthermore, the introduction of p27 inhibits cell-cycle progression even in the presence of forskolin. These data suggest that PKA promotes cell proliferation upstream of the interaction between cyclin D1 and p27. It was reported that cyclin D1 is a direct target of Wnt/β-catenin signalling (Tetsu and McCormick, 1999; Shtutman et al., 1999). We found that Δ47-β-catenin promotes the proliferation of retinal cells in zebrafish, and that ΔN-Tcf3 inhibits the proliferation of retinal cells induced by forskolin treatment. These data suggest that Wnt/β-catenin signalling is required for PKA-mediated proliferation. However, dnPKA does not suppress Wnt-induced overproliferation, suggesting that a high level of Wnt activity maintains cell proliferation in the absence of PKA activity. Together, these data suggest that PKA plays a supplemental

role in Wnt-induced proliferation, or that PKA inhibits exit from Wnt-mediated cell-cycle progression rather than promoting cell-cycle progression in concert with Wnt signalling.

What is the molecular mechanism that underlies PKA-mediated inhibition of retinal neurogenesis? There are two possible pathways (Fig. 8A). One possibility is that PKA inhibits the expression of the cdk inhibitor *p27*. Because PKA antagonises the Hh signalling pathway, Hh-mediated Gli activation may be required for *p27* expression in the zebrafish retina. Although it is unknown whether Gli transcription factors directly regulate the transcription of *p27*, the activator form of Gli may positively regulate the expressison of *p27*. It was reported that Indian Hh induces colonic epithelial differentiation by antagonising Wnt/β-catenin signalling (van den Brink et al., 2004). In this case, Hh signalling is required for activation of the cdk inhibitor Cip1/Waf1/p21, and negatively regulates cyclin D1, suggesting that a common mechanism may regulate both zebrafish retinal neurogenesis and mouse colonic epithelial differentiation. Although Gli-MO injection induces severe defects in the progression of neuronal production, it is also possible that PKA promotes cell proliferation though Gli-independent pathway. One of the major PKA substrates, CREB, binds to the promoter of cell-cycle regulators such as cyclin D1 (Lonze and Ginty, 2002). PKA phosphorylates Ser133 of CREB and this phosphorylated form of CREB recruits p300/CBP histone acetyltransferase (HAT) to activate the transcription of *cyclin D1*. As ΔN-Tcf3 inhibits cell-cycle progression in the presence of forskolin, phophorylated CREB may activate the transcriptional activity of Tcf3/β-catenin complex in this model. We show that forskolin treatment does not activate transcription under the control of the β-catenin responsive promoter (Fig. 3K). However, this is not contradictory to this model, because the β-catenin responsive promoter does not contain the CREB-binding sequence. In the developing mouse cerebellum, Shh induces G1-S transition to promote proliferation of granule cell precursors (Wechsler-Reya and Scott, 1999), whereas an extracellular matrix protein, Vitronectin, promotes granule cell differentiation through PKA-mediated CREB phosphorylation (Pons et al., 2001). As Shh suppresses PKA-mediated CREB phosphorylation in cerebellar development, competition between the Shh and PKA-CREB pathway determines whether granule cell precursors continue to proliferate or whether they differentiate. Although the role of Hh in cerebellar development is the reverse of that in zebrafish retinal development, the PKA-CREB pathway may be involved in the switch between proliferation and differentiation in the zebrafish retina.

Forskolin treatment inhibits retinal neurogenesis more severely than cyclopamine treatment or the *smu* mutation

The progression of neuronal production is completely inhibited in the presence of forskolin, but is only delayed in the *smu* mutant and following cyclopamine treatment. Milder defects in *ath5* expression in *smu* mutant retinas may be due to maternal Smu activity. However, the delay of neurogenesis in the presence of cyclopamine is difficult to explain by such redundancy. One possibility is that cyclopamine treatment is insufficient to block Hh signalling completely. Recently, it was

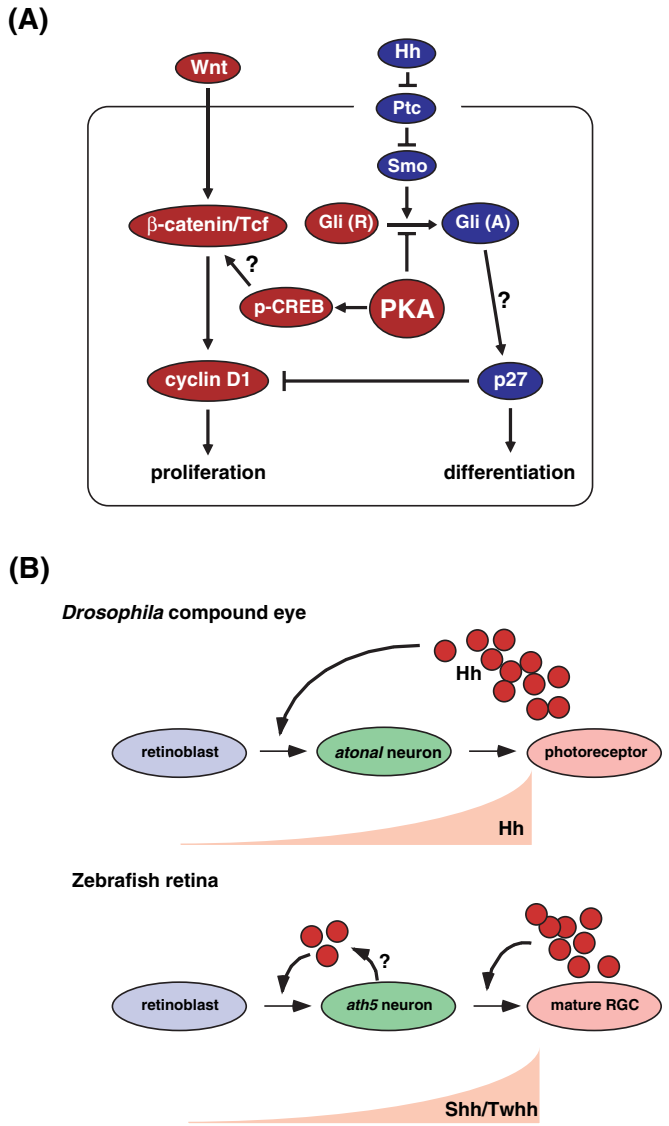

Fig. 8. Hh-PKA signalling regulates two steps of RGC differentiation in zebrafish. (A) Model for PKA-mediated inhibition of the cell-cycle exit of retinoblasts. PKA interacts with both the Hh and the Wnt signalling pathway. PKA inhibits Hh-mediated Gli activation. The activator form of Gli may promote the expression of *p27*. Another possible pathway is that PKA promotes the phosphorylation of Ser133 of CREB. This phosphorylation may activate the transcriptional activity of the β-catenin/Tcf3 complex to elevate the expression of *cyclin D1*. (B) Model of Hh actions in the *Drosophila* compound eye and the zebrafish retina. In *Drosophila*, Hh is expressed in photoreceptors and acts on adjacent retinoblasts to induce the proneural gene *atonal*, which promotes the differentiation of photoreceptors. Thus, a single cycle of Hh activation and cell differentiation advances the neurogenic wave across the fly eye. By contrast, in zebrafish Hh signalling regulates at least two steps of RGC differentiation: the cell-cycle-exit of retinoblasts and the maturation of RGCs. Shh or Twhh acts as a short-range signal to induce the cell-cycle exit of retinoblasts and *ath5* expression. *ath5*-positive cells located in the wave front may be a source of Hh signals. In the later stages, *ath5*-positive neurons differentiate into mature RGCs and express high levels of Shh/Twhh, which act on adjacent *ath5*-positve neurons causing them to differentiate into mature RGCs. In this model, dual cycles of Hh activation and cell differentiation cooperatively regulate the differentiation of RGCs.

reported that cyclopamine has a relatively low affinity for Smo (Williams et al., 2003; Romer et al., 2004). Furthermore, cyclopamine is hydrophobic chemical. These characteristics may result in an incomplete inhibition of Hh signalling. An alternative possibility is that the blockade of Smo function is not sufficient to inhibit the progression of neuronal production in the zebrafish retina. Western blotting with an antibody against phosphorylated CREB suggests that the level of PKA activity is much higher in forskolin-treated embryos than in wild-type and *smu* mutant embryos. The level of PKA activity may correlate with the severity of defects in *ath5* expression. Although it still remains to be elucidated how PKA inhibits the Hh signalling pathway in vertebrates, it is generally accepted that PKA negatively regulates Hh-dependent Gli activation by promoting the cytoplasmic sequestration of Gli1 and generating the repressor forms of Gli2 and Gli3 (Ingham and McMahon, 2001). It is possible that the ratio of the repressor form to the activator form of Gli proteins is higher following forskolin treatment than it is following cyclopamine treatment or in *smu* mutants. High predominance of repressor activity over activator activity may be necessary to inhibit progression of neuronal production. This idea seems to be supported by our observation that progression of neuronal production is more severely affected in Gli-MO-injected retinas than in *smu* mutant retinas (Fig. 4M). Another possibility is that the activation of CREB contributes to the forskolin-induced defects in neuronal production. Because phosphorylation of CREB by PKA activates the transcription of *cyclin D1* (Lonze and Ginty, 2002), CREB-mediated activation of *cyclin D1* expression may inhibit the cell-cycle exit of retinoblasts in concert with the blockade of Hh-mediated Gli activation.

Hh signalling regulates two distinct steps of RGC differentiation

A previous study suggested that *shh* is expressed in RGCs and induces neighbouring uncommitted cells to differentiate into RGCs (Neumann and Nuesslein-Volhard, 2000). In this study, we show that Hh signalling promotes mitotic retinoblasts to generate postmitotic daughter cells. These results raise the possibility that Hh signals emanating from RGCs induce adjacent mitotic cells to generate neurons that become RGCs and function as a new source of Hh signals. However, the wave front of *ath5* expression reaches the temporal retina at 27 hpf, before the first differentiated RGC starts axonogenesis (Laessing and Stuermer, 1996), which suggests that mature RGCs are not the source of Hh signals. Furthermore, this early spread of *ath5* expression seems contradictory to the previous observation that blockade of Hh signalling by cyclopamine after 26 hpf strongly inhibits the progression of RGC differentiation (Neumann and Nuesslein-Volhard, 2000). These data suggest that the wave of *ath5* expression does not strongly correlate with that of RGC differentiation. In this study, we show that forskolin treatment after 27 hpf has no effect on the progression of *ath5* expression, but that it does inhibit the progression of markers of mature RGCs. These data suggest that Hh signalling regulates two distinct steps of RGC differentiation: the cell-cycle exit of retinoblasts and the progression of *ath5*-positive neurons into mature RGCs. Considering the time lag between forskolin treatment and the inhibition of Hh signalling, Hh signalling after 29 hpf does not regulate the progression of *ath5* expression but does regulate the progression of RGC differentiation (Fig. 6N). After 29 hpf, Hh may promote the progression of uncommitted postmitotic neurons into mature RGCs. This later requirement of the Hh signalling pathway for RGC differentiation is consistent with the previous observation of Neumann and Nuesslein-Volhard (Neumann and Nuesslein-Volhard, 2000).

In this study, we show that only forskolin treatment completely inhibits the progression of neuronal production; the progression of neuronal production is only delayed following cyclopamine treatment or in the *smu* mutation (Stenkamp and Frey, 2003). However, it was reported that the progression of RGC maturation is severely inhibited by treatment with cyclopamine (Neumann and Nuesslein-Volhard, 2000). These observations suggest that mild blockade of Hh signalling is sufficient to inhibit the progression of RGC maturation, whereas severe blockade of Hh signalling is necessary to inhibit the progression of neuronal production. If this is the case, it is possible that a low dose of Hh signals is sufficient to induce the cell-cycle exit of retinoblasts, while a high dose of Hh signals is necessary to promote the progression of *ath5*-positive cells into mature RGCs. This idea seems to be consistent with a model proposing that early differentiating cells near the wave front of neuronal production express a low level of Hh, which acts on adjacent retinoblasts causing them to exit from the cell cycle, and that mature RGCs express a high level of Hh, which acts on adjacent uncommitted neurons causing them to differentiate into mature RGCs (Fig. 8B).

What is the significance of such dual regulation of Hh signalling in RGC differentiation? Initial Hh signalling generates *ath5*-positive neurons, which might be uncommitted to any retinal cell-types. Later Hh signalling promotes *ath5*-positive neurons to differentiate into RGCs. It is possible that some *ath5*-positive neurons do not respond to the later Hh signals and differentiate into other types of retinal cells, such as amacrine cells. If this is the case, the dual actions of Hh play a role in the generation of diversity of retinal cell-types through the maintenance of a pool of uncommitted neurons. As another possibility, a pool of uncommitted neurons may be useful to regulate the number of RGCs during development. The most recent study revealed that Shh is expressed in amacrine cells and directs the differentiation and lamination of the inner and outer nuclear layers (Shkumatava et al., 2004). Although the authors showed that Shh expression in amacrine cells is independent of RGC differentiation, it is unknown whether Shh expression in amacrine cells requires the initial action of Hh signals that mediate cell-cycle exit of retinoblasts. In the future, it will be important to elucidate whether *shh*-expressing amacrine cells are generated from a pool of *ath5*-positive neurons.

Short-range action of Shh and Twhh regulates the progression of *ath5* expression in zebrafish

Pulse treatment results suggest that Hh signalling between 24 and 29 hpf is required for the wave of *ath5* expression (Fig. 6N). Furthermore, the introduction of *shh* and *twhh* morpholino-antisense oligonucleotides blocks neuronal production in the retina. These data suggest that Shh and Twhh regulate the progression of *ath5* expression between 24 and 29 hpf. However, it is difficult to detect *shh* and *twhh* mRNA expression in the neural retina at this early stage, although it was reported that *shh* RNA is expressed in the retina at 28 hpf

(Neumann and Nuesslein-Volhard, 2000). One possibility is that Shh and Twhh expressed in the ventral forebrain may have a long-range action on progenitor cells of the optic cup. It was reported that Hh expressed in midline tissue is important for proliferation of the developing forebrain in chicks and mice, probably through its long-range actions (Britto et al., 2002; Ishibashi and McMahon, 2002). The most recent study on Hh signalling in the zebrafish retina also suggested that Hh signalling outside the optic cup regulates *ath5* expression before 27 hpf (Stenkamp and Frey, 2003). However, we do not consider this as the most likely explanation, as the wave of *ath5* expression normally occurs when the optic cups are dissected from the forebrain at 18 hpf, and cultured as an explant later (Masai et al., 2000), suggesting that a source of Hh signals is localised within the optic cup. Furthermore, when the dissected eye cup was divided into two (the nasal and temporal halves) only the nasal half expressed *ath5* (Masai et al., 2000), suggesting that short-range Hh signalling acts from the nasal to temporal regions across the neural retina. Transplantation of hh-MO-injected cells into wild-type host retinas demonstrated that *ath5* expression is rarely observed in hh-MO-injected retinal columns, and that wild-type cells fail to express *ath5* when they are located adjacent to the temporal side of Shh- and Twhh-deprived cells. These data suggest that a short-range action of Shh and Twhh expressed in the neural retina regulates the wave of *ath5* expression and neuronal production. Low levels of Shh and Twhh expression may spread to the temporal retina up until 27 hpf and may be sufficient to regulate the wave of *ath5* expression.

Does Hh function as a mitogen or an anti-mitogen in the vertebrate retina?

In this study, we propose that Hh signals induce the cell-cycle exit of retinal progenitor cells. However, several studies have suggested that Hh functions as a mitogen for neural stem cells in the retina and in the brain, for astrocyte precursor cells in the optic stalk, and for granule cell precursors in the cerebellum (Roy and Ingham, 2002; Ruiz i Altaba et al., 2002). The observation of such an opposite phenotype may be due to the difference in cell types or the species used in the studies. Otherwise, as discussed previously (Yang, 2004), the difference in the dose of Hh signals may cause the opposite behaviour of retinal progenitor cells. For example, a low dose of Hh signals as an anti-mitogen promotes neuronal production, whereas a high dose of Hh signals inhibits the differentiation of early-born cell types to maintain a pool of mitotic cells for the generation of late-born cell types. In *Drosophila* eyes, Hh regulates not only neuronal differentiation by inducing the proneural gene *atonal*, but also proliferation by inducing *cyclin D/E* (Duman-Scheel et al., 2002). Such dual roles of Hh as a mitogen and an anti-mitogen may coordinate proliferation with cell differentiation in the vertebrate retina.

The mitogenic role of Hh has been proposed from in vitro experiments carried out using cell pellets or explant culture. Recent in vivo analyses of the role of Hh in the vertebrate retina showed different phenotypes of retinal neurogenesis. In conditional *shh* knock-out mice, Müller glial cells fail to differentiate properly and the outer photoreceptor layer shows a rosette structure (Wang et al., 2002). In frog retina treated with the Hh inhibitor cyclopamine, retinal progenitor cells are normal and only differentiation of the pigmented epithelium is perturbed (Perron et al., 2003). We could not detect any defects in the differentiation of the pigment epithelium in zebrafish embryos treated with forskolin or in $smu^{-/-}$ embryos. The roles of Hh signalling in retinal development may be diverse among different species of vertebrates. In the future, it will be important to elucidate why retinal cells show such different behaviours in response to Hh signals.

We thank Dr Steve Devoto for providing smu^{b577} fish, Dr Carl Neumann for the transgenic fish Tg(shh:GFP), Dr Randall Moon for the dnPKA construct and the TOPdGFP transgenic fish, Dr Shin-ichi Ohnuma for *Xenopus* p27 cDNA, and Dr Ajay B. Chitnis for the ΔN-Tcf3 construct. This study was supported by a RIKEN BSI grant to H.O. and funds from RIKEN Initiative Research Unit and PRESTO, JST to I.M.

References

Barresi, M. J. F., Stickney, H. L. and Devoto, S. H. (2000). The zebrafish *slow-muscle-omitted* gene product is required for Hedgehog signal transduction and the development of slow muscle identity. *Development* **127**, 2189-2199.

Britto, J., Tannahill, D. and Keynes, R. (2002). A critical role for sonic hedgehog signaling in the early expansion of the developing brain. *Nat. Neurosci*. **5**, 103-110.

Chen, J. K., Taipale, J., Cooper, M. K. and Beachy, P. A. (2002). Inhibition of Hedgehog signaling by direct binding of cyclopamine to Smoothened. *Genes Dev.* **16**, 2743-2748.

Chenn, A. and Walsh, C. A. (2002). Regulation of cerebral cortical size by control of cell cycle exit in neural precursors. *Science* **297**, 365-369.

Chuang, J. C., Mathers, P. H. and Raymond, P. A. (1999). Expression of three *Rx* homeobox genes in embryonic and adult zebrafish. *Mech. Dev*. **84**, 195-198.

Cohen, M. M., Jr (2003). The hedgehog signaling network. *Am. J. Med. Genet*. **123A**, 5-28.

Concordet, J.-P., Lewis, K. E., Moore, J. W., Goodrich, L. V., Johnson, R. L., Scott, M. P. and Ingham, P. W. (1996). Spatial regulation of a zebrafish *patched* homologue reflects the roles of *sonic hedgehog* and protein kinase A in neural tube and somite patterning. *Development* **122**, 2835-2846.

Cooper, M. K., Porter, J. A., Young, K. E. and Beachy, P. A. (1998). Teratogen-mediated inhibition of target tissue response to *Shh* signaling. *Science* **280**, 1603-1607.

Dorsky, R. I., Sheldahl, L. C. and Moon, R. T. (2002). A transgenic Lef1/β-catenin-dependent reporter is expressed in spatially restricted domains throughout zebrafish development. *Dev. Biol*. **241**, 229-237.

Dowling, J. (1987). *The Retina.* Cambridge, MA: Harvard University Press.

Duman-Scheel, M., Weng, L., Xin, S. and Du, W. (2002). Hedgehog regulates cell growth and proliferation by inducing Cyclin D and Cyclin E. *Nature* **417**, 299-304.

Dyer, M. A. and Cepko, C. L. (2001). Regulating proliferation during retinal development. *Nat. Rev. Neurosci*. **2**, 333-342.

Fantl, V., Stamp, G., Andrews, A., Rosewell, I. and Dickson, C. (1995). Mice lacking cyclin D1 are small and show defects in eye and mammary gland development. *Genes Dev*. **9**, 2364-2372.

Galderisi, U., Jori, F. P. and Giordano, A. (2003). Cell cycle regulation and neuronal differentiation. *Oncogene* **22**, 5208-5219.

Geng, Y., Yu, Q., Sicinska, E., Das, M., Bronson, R. T. and Sicinski, P. (2001). Deletion of the $p27^{Kip1}$ gene restores normal development in cyclin D1-deficient mice. *Proc. Natl. Acad. Sci. USA* **98**, 194-199.

Glasgow, E., Karavanov, A. A. and Dawid, I. B. (1997). Neuronal and neuroendcrine expression of *lim3*, a LIM class homeobox gene, is altered in mutant zebrafish with axial signaling defects. *Dev. Biol*. **192**, 405-419.

Halloran, M. C., Sato-Maeda, M., Warren, J. T., Su, F., Lele, Z., Krone, P. H., Kuwada, J. Y. and Shoji, W. (2000). Laser-induced gene expression in specific cells of transgenic zebrafish. *Development* **127**, 1953-1960.

Hammerschmidt, M., Bitgood, M. J. and McMahon, A. P. (1996). Protein kinase A is a common negative regulator of Hedgehog signaling in the vertebrate embryo. *Genes Dev*. **10**, 647-658.

Hu, M. and Easter, S. S., Jr (1999). Retinal neurogenesis: the formation of the initial central patch of postmitotic cells. *Dev Biol*. **207**, 309-321.

Ingham, P. W. and McMahon, A. P. (2001). Hedgehog signaling in animal development: paradigms and principles. *Genes Dev*. **15**, 3059-3087.

Inoue, A., Takahashi, M., Hatta, K., Hotta, Y. and Okamoto, H. (1994). Developmental regulation of Islet-1 mRNA expression during neuronal differentiation in embryonic zebrafish. *Dev. Dyn*. **199**, 1-11.

Ishibashi, M. and McMahon, A. P. (2002). A sonic hedgehog-dependent signaling relay regulates growth of diencephalic and mesencephalic primordia in the early mouse embryo. *Development* **129**, 4807-4819.

Karlstrom, R. O., Tyurina, O. V., Kawakami, A., Nishioka, N., Talbot, W. S., Sasaki, H. and Schier, A. F. (2003). Genetic analysis of zebrafish *gli1* and *gli2* reveals divergent requirements for *gli* genes in vertebrate development. *Development* **130**, 1549-1564.

Kay, J. N., Finger-Baier, K. C., Roeser, T., Staub, W. and Baier, H. (2001). Retinal ganglion cells genesis requires *lakritz*, a zebrafish *atonal* homolog. *Neuron* **30**, 725-736.

Kim, C.-H., Oda, T., Itoh, M., Jiang, D., Artinger, K. B., Chandrasekharappa, S. C., Driever, W. and Chitnis, A. B. (2000). Repressor activity of Headless/Tcf3 is essential for vertebrate head formation. *Nature* **407**, 913-916.

Kubo, F., Takeichi, M. and Nakagawa, S. (2003). Wnt2b controls retinal cell differentiation at the ciliary marginal zone. *Development* **130**, 587-598.

Kumar, J. P. (2001). Signalling pathways in *Drosophila* and vertebrate retinal development. *Nat. Rev. Genet.* **2**, 846-857.

Laessing, U. and Stuermer, C. A. O. (1996). Spatiotemporal pattern of retinal ganglion cell differentiation revealed by the expression of neurolin in embryonic zebrafish. *J. Neurobiol.* **29**, 65-74.

Levine, E. M. and Green, E. S. (2004). Cell-intrinsic regulators of proliferation in vertebrate retinal progenitors. *Semi. Cell Dev. Biol*. **15**, 63-74.

Livesey, F. J. and Cepko, C. L. (2001). Vertebrate neural cell-fate determination: lessons from the retina. *Nat. Rev. Neurosci*. **2**, 109-118.

Lonze, B. E. and Ginty, D. D. (2002). Function and regulation of CREB family transcription factors in the nervous system. *Neuron* **35**, 605-623.

Macdonald, R., Barth, K. A., Xu, Q., Holder, N., Mikkola, I. and Wilson, S. W. (1995). Midline signalling is required for Pax gene regulation and patterning of the eyes. *Development* **121**, 3267-3278.

Marquardt, T. and Gruss, P. (2002). Generating neuronal diversity in the retina: one for nearly all. *Trends Neurosci*. **25**, 32-38.

Masai, I., Stemple, D. L., Okamoto, H. and Wilson, S. W. (2000). Midline signals regulate retinal neurogenesis in zebrafish. *Neuron* **27**, 251-263.

Masai, I., Lele, Z., Yamaguchi, M., Komori, A., Nakata, A., Nishiwaki, Y., Wada, H., Tanaka, H., Nojima, Y., Hammerschmidt et al. (2003). N-cadherin mediates retinal lamination, maintenance of forebrain compartments and patterning of retinal neuritis. *Development* **130**, 2479-2494.

Murray, A. W. (2004). Recycling the cell cycle: cyclins revisited. *Cell* **116**, 221-234.

Nasevicius, A. and Ekker, S. C. (2000). Effective targeted gene 'knockdown' in zebrafish. *Nat. Genet*. **26**, 216-220.

Neumann, C. J. and Nuesslein-Volhard, C. (2000). Patterning of the zebrafish retina by a wave of Sonic Hedgehog activity. *Science* **289**, 2137-2139.

Ohnuma, S. and Harris, W. A. (2003). Neurogenesis and the cell cycle. *Neuron* **40**, 199-208.

Ohnuma, S., Hopper, S., Wang, K. C., Philpott, A. and Harris, W. A. (2002). Co-ordinating retinal histogenesis: early cell cycle exit enhances early cell fate determination in the *Xenopus* retina. *Development* **129**, 2435-2446.

Perron, M., Boy, S., Amato, M. A., Viczian, A., Koebernick, K., Pieler, T. and Harris, W. A. (2003). A novel function for *Hedgehog* signalling in retinal pigment epithelium differentiation. *Development* **130**, 1565-1577.

Pons, S., Trejo, J. L., Martínez-Morales, J. R. and Martí, E. (2001). Vitronectin regulates Sonic hedgehog activity during cerebellum development through CREB phosphorylation. *Development* **128**, 1481-1492.

Pujic, Z. and Malicki, J. (2004). Retinal pattern and the genetic basis of its formation in zebrafish. *Semi. Cell Dev. Biol*. **15**, 105-114.

Radtke, F. and Raj, K. (2003). The role of Notch in tumorigenesis: oncogene or tumor suppressor? *Nat. Rev. Cancer* **3**, 756-767.

Romer, J. T., Kimura, H., Magdaleno, S., Sasai, K., Fuller, C., Baines, H., Connelly, M., Stewart, C. F., Gould, S., Rubin, L. L. and Curran, T. (2004). Suppression of the Shh pathway using a small molecule inhibitor eliminates medulloblastoma in $Ptc^{+/-}p53^{-/-}$ mice. *Cancer Cell* **6**, 229-240.

Roy, S. and Ingham, P. W. (2002). Hedgehogs tryst with the cell cycle. *J. Cell Sci.* **115**, 4393-4397.

Ruiz i Altaba, A., Palma, V. and Dahmane, N. (2002). Hedgehog-Gli signalling and the growth of the brain. *Nat. Rev. Neurosci*. **3**, 24-33.

Rupp, R. A. W., Snider, L. and Weintraub, H. (1994). *Xenopus* embryos regulate the nuclear localization of XmyoD. *Genes Dev*. **8**, 1311-1323.

Russell, C. (2003). The roles of Hedgehogs and Fibroblast Growth Factors in eye development and retinal cell rescue. *Vision Res*. **43**, 899-912.

Schmitt, E. A. and Dowling, J. E. (1996). Comparison of topographical patterns of ganglion and photoreceptor cell differentiation in the retina of the zebrafish, *Danio rerio*. *J. Comp. Neurol*. **371**, 222-234.

Shkumatava, A., Fisher, S., Müller, F., Strahle, U. and Neumann, C. J. (2004). Sonic hedgehog, secreted by amacrine cells, acts as a short-range signal to direct differentiation and lamination in the zebrafish retina. *Development* **131**, 3849-3858.

Shtutman, M., Zhurinsky, J., Simcha, I., Albanese, C., D'Amico, M., Pestell, R. and Ben-Zéev, A. (1999). The cyclin D1 gene is a target of the β-catenin/LEF-1 pathway. *Proc. Natl. Acad. Sci. USA* **96**, 5522-5527.

Sicinski, P., Donaher, J. L., Parker, S. B., Li, T., Fazeli, A., Gardner, H., Haslam, S. Z., Bronson, R. T., Elledge, S. J. and Weinberg, R. A. (1995). Cyclin D1 provides a link between development and oncogenesis in the retina and breast. *Cell* **82**, 621-630.

Stenkamp, D. L., Frey, R. A., Prabhudesai, S. N. and Raymond, P. A. (2000). Function for *Hedgehog* genes in zebrafish retinal development. *Dev. Biol*. **220**, 238-252.

Stenkamp, D. L. and Frey, R. A. (2003). Extraretinal and retinal hedgehog signaling sequentially regulate retinal differentiation in zebrafish. *Dev. Biol*. **258**, 349-363.

Su, J. Y., Rempel, R. E., Erikson, E. and Maller, J. L. (1995). Cloning and characterization of the *Xenopus* cyclin-dependent kinase inhibitor $p27^{XIC1}$. *Proc. Natl. Acad. Sci. USA* **92**, 10187-10191.

Tetsu, O. and McCormick, F. (1999). β-Catenin regulates expression of cyclin D1 in colon carcinoma cells. *Nature* **398**, 422-426.

Ungar, A. R. and Moon, R. T. (1996). Inhibition of protein kinase A phenocopies ectopic expression of *hedgehog* in the CNS of wild-type and *cyclops* mutant embryos. *Dev. Biol.* **178**, 186-191.

van den Brink, G. R., Bleuming, S. A., Hardwick, J. C. H., Schepman, B. L., Offerhaus, G. J., Keller, J. J., Nielsen, C., Gaffield, W., van Deventer, S. J. H., Roberts, D. J. et al. (2004). Indian Hedgehog is an antagonist of Wnt signaling in colonic epithelial cell differentiation. *Nat. Genet*. **36**, 277-282.

van Es, J. H., Barker, N. and Clevers, H. (2003). You Wnt some, you lose some: oncogenes in the Wnt signaling pathway. *Curr. Opin. Genet. Dev.* **13**, 28-33.

Varga, Z. M., Amores, A., Lewis, K. E., Yan, Y.-L., Postlethwait, J. H., Eisen, J. S. and Westerfield, M. (2001). Zebrafish *smoothened* functions in ventral neural tube specification and axon tract formation. *Development* **128**, 3497-3509.

Wang, Y. P., Dakubo, G., Howley, P., Campsall, K. D., Mazarolle, C. J., Shiga, S. A., Lewis, P. M., McMahon, A. P. and Wallace, V. A. (2002). Development of normal retinal organization depends on Sonic hedgehog signaling from ganglion cells. *Nat. Neurosci*. **5**, 831-832.

Wechsler-Reya, R. J. and Scott, M. P. (1999). Control of neuronal precursor proliferation in the cerebellum by Sonic Hedgehog. *Neuron* **22**, 103-114.

Wei, Y. and Allis, C. D. (1998). Pictures in cell biology. *Trends Cell Biol*. **8**, 226.

Williams, J. A., Guicherit, O. M., Zaharian, B. I., Xu, Y., Chai, L., Wichterle, H., Kon, C., Gatchalian, C., Porter, J. A., Rubin, L. L. and Wang, F. Y. (2003). Identification of a small molecule inhibitor of the hedgehog signaling pathway: Effects on basal call carcinoma-like lesions. *Proc. Natl. Acad. Sci. USA* **100**, 4616-4621.

Yang, X.-J. (2004). Roles of cell-extrinsic growth factors in vertebrate eye pattern formation and retinogenesis. *Semin. Cell Dev. Biol*. **15**, 91-103.

Yarden, A., Salomon, D. and Geiger, B. (1995). Zebrafish cyclin D1 is differentially expressed during early embryogenesis. *Biochim. Biophys. Acta*. **1264**, 257-260.